Hyindoor

Pre-normative research on safe indoor use of fuel cells and hydrogen systems

Small or medium-scale focused research project
Joint Technology Initiatives – Collaborative project (FCH)

Contract Number: 278534
Start date: 02/01/2012 Duration: 36 Months

New Energy World JU
fuel cells & hydrogen for sustainability

Work Package 5: Widely accepted guidelines on Fuel Cell indoor installation and use

D5.1

Hyindoorproject–Contract Number: 278534
Pre-normative research on safe indoor use of fuel cells and hydrogen systems

Document type	Deliverable
Work Package	WP 5
Document number	D5.1 – summary draft
Dissemination level	Restricted to the partners of the Hyindoor project

Revisions

Rev.	Authors	WP Leader - signature	Project Coordinator - signature
0	D. Houssin Air Liquide 2014/01		
1	D. Houssin, B. Chernyavsky, V. Molkov, S. Jallais, V. Shentsov, R. Dey		
2	D. Houssin, B. Chernyavsky, V. Molkov, S. Jallais, V. Shentsov, R. Dey, P. Hooker		
3-5	D. Houssin, B. Chernyavsky, V. Molkov, S. Jallais, V. Shentsov, D. Makarov, R. Dey, P. Hooker, V. Palmisano, E Weidner, D. Baraldi, D. Melideo		
6	AL, UU, JRC		

Distribution

Name	Organisation	Comments
FCH-JU ProjectOfficer	FCH-JU	
All beneficiaries	Hyindoor	Through the collaborative work space

Table of contents

Figures & Tables

List of figures

List of tables

1. Introduction

The objective of this document is to provide guidelines and best practices easily usable by engineers for indoor safely use of hydrogen energy applications.

Four main topics were addressed in Hyindoor project:

- Hydrogen release inside a confined or semi-confined enclosure,
- Indoor hydrogen-air deflagration,
- Jet fire and underventilated fire,
- Hydrogen detection for confined spaces.

These topics were studied through:

- A review of the state of the art on published information and critically analyzed,
- Targeted experiments specifically performed in Hyindoor project,
- Evaluation and validation of analytical and numerical approaches to assess phenomena.

General rules, best practices and means to assess and mitigate consequences are proposed in this document.

2. Hyindoor project contributions

2.1 General safety strategies for inherently safer hydrogen use indoors

2.1.1 Safety objectives of H_2 use indoor

There are three generic safety objectives for any safety system including for use of hydrogen systems indoors:

- Life Safety
- Property protection
- Environment protection

Primary consideration should be given to life safety, including site workers, customers and general public. Harm criteria for humans are presented in Appendix 4.1.1. The **life safety** objectives may include, but not limited to (Saffers and Molkov, 2014):

a) The occupants are able to leave building/facility in reasonable time, or consequences to occupants are acceptably low;
b) First responders are able to operate in reasonable safety;
c) Collapse or debris does not endanger bystanders, first responders and other people likely to be near facility.

Facility owners should give consideration to reducing of the damage to infrastructure structures and equipment and to minimise disruption of business, preserve corporate image and reduce direct and indirect financial losses. Attention should be paid to preventing the escalating effects of objects, events and layouts on damages and to value and importance of the property in and around a facility (Saffers and Molkov, 2014).

Local authorities and regulators should be involved in the estimation of environment impact from accidents involving hydrogen for:

a) Prevention of significant damage to neighbouring facilities and reduction of “domino effect”;
b) Limit adverse effects on the natural environment, such as asphyxiation and cold burns on fauna and flora.

2.1.2 Phenomena and consequences diagram

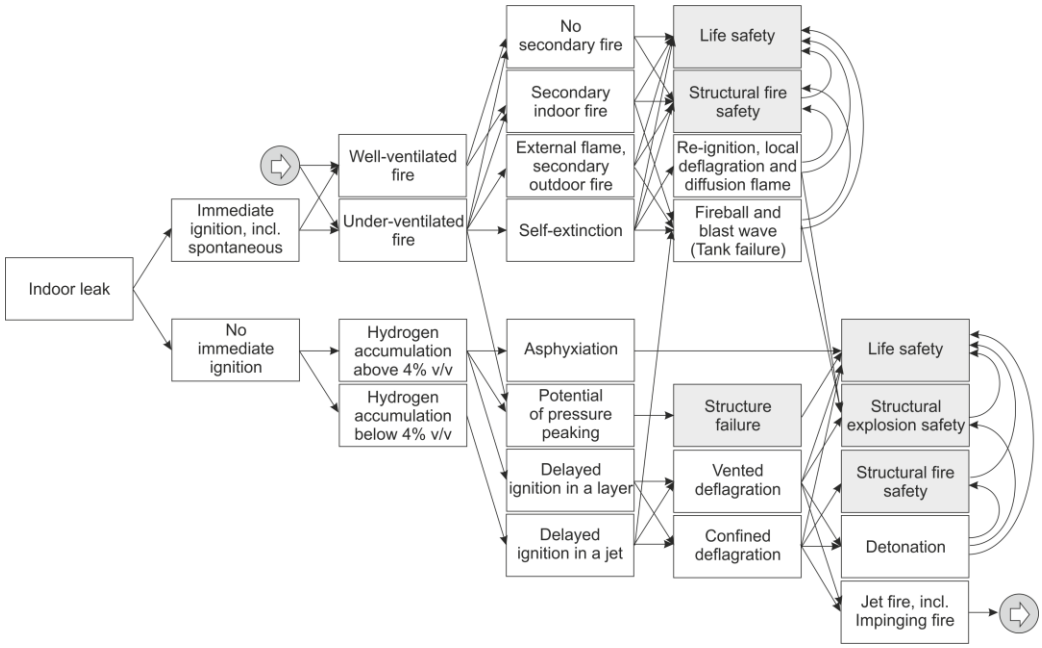

Figure 1. Phenomena and consequences diagram. White boxes - various phenomena, starting with the development of hydrogen leak. Grey boxes - potential consequences. Note that even if no immediate ignition has occurred (lower branch), subsequent chain of events can lead to delayed ignition leading to transition to the upper branch, as indicated by arrow in a circle pictograms.

Safety relevant phenomena and potential consequences associated with indoor incidents/accidents involving hydrogen systems and infrastructure are summarized in the diagram in Figure 1.

The event starts with the **indoor hydrogen leak**. Depending whether released hydrogen **ignites immediately upon release**, subsequent development can follow two possible scenarios. The ignition can be caused by the presence of open fire, hot surface, electric or mechanical sparking and other factors, as well as hydrogen-specific phenomenon **of spontaneous ignition by so-called "diffusion" mechanism (see e.g. Molkov, 2012).**

If immediate ignition had occurred, e.g. by spontaneous ignition within piping filled with air, subsequent fire can develop in two distinctive modes: **well-ventilated** and **under-ventilated**. Well-ventilated fire is characterized by a relatively low hydrogen release rate and complete combustion of hydrogen within the enclosure. Hazards to life during well-ventilated fire include direct effect from flame and hot combustion products current, radiation from hot layer under the ceiling and hot solid surfaces like roof, structural failure of load bearing construction elements due to direct impingement flame, etc. Increase in hydrogen release rate can result in transition to under-ventilated fire regime, when oxygen is consumed at a faster rate than it can be replenished through ventilation if possible at all. Under-ventilated fire can result in two sub-regimes – development of **an external flame** occurring in the vents (with no combustion inside) and full **self-extinction** of fire within and without enclosure. Care should be taken that after self-extinction of fire, e.g. in a fuel cell container, hydrogen is not accumulated above hazardous limit in enclosure accommodating the fuel cell.

Both types of fire can result in the ignition of combustible objects and flammable substances inside the enclosure, producing **secondary indoor fire**. This can lead to fire continuing burning even after the cessation of hydrogen release, e.g. due to shutting of safety valves, and additional hazards, such as release of toxic smoke. Under-ventilated fire is characterised by comparatively large hydrogen release rate. Thus, there is a potential for **pressure peaking phenomenon**, endangering structural integrity of the enclosure (Brennan and Molkov, 2013). Consequently, overpressure due to pressure peaking phenomenon should be assessed as a part of safety engineering design (see Appendix 4.2.1). It is worth noting that both unignited and ignited releases can generate hazardous overpressure due to pressure peaking phenomenon. However, calculation of overpressure is different for unignited release and jet fire. Under-ventilated fire resulting in an external flame can also produce **secondary outdoor fire**.

If left burning sufficiently long, both types of fires, as well as secondary fires can lead to a failure of storage tank(s), resulting in a fast energy release and ignition of large quantities of hydrogen, producing **fireball** and **blast wave**. External flame and secondary outdoor fires can also result in failure of outside storage tank(s). Measures should be taken to prevent this, e.g. by placing external hydrogen storage far from enclosure vents.

An under-ventilated fire that undergoes self-extinction can be **re-ignited** if a fresh supply of air would enter the enclosure. It can potentially lead to a **localized deflagration** and **diffusion flame** in the zones containing hydrogen above the Lower Flammability Limit (LFL).

All type of fires present life **safety hazards**, including direct thermal damage from the flame, radiation thermal damage, overpressure due to the pressure peaking phenomenon, and potentially poisoning by the toxic combustion products produced by secondary fires.

Fires of all types also present **structural fire safety** hazard, as prolonged fire within the enclosure can result in weakening of its structural integrity and eventual collapse of the enclosure.

If hydrogen leak will not ignite immediately upon release, it would lead to a gradual **hydrogen accumulation** within the enclosure. High flow rate release exceeding ventilation capacity can produce hydrogen **concentration exceeding 4%** by volume, i.e. LFL, which creates possibility for **delayed ignition in a layer and its deflagration**. Furthermore, high flow rate release can result in **asphyxiation** and **pressure peaking phenomenon**. While hydrogen itself is not poisonous, it does not support metabolism either. As with any gas (except oxygen) a risk of asphyxiation exists mainly in confined areas as a result of oxygen depletion (ISO/TPRD 15916, 2008). Proper ventilation system should exclude any life threat including asphyxiation.

Lower hydrogen release rates which do not produce accumulated hydrogen concentration above 4% in a layer can still result in a **delayed ignition in a jet**. Both types of delayed ignition can result in deflagration of hydrogen-air mixture with overpressure able to destroy he enclosure. Mitigation of explosions by venting of deflagration is the most wide spread technique (see Appendix 4.3.2). When the enclosure possess openings (vents) allowing deflagration overpressure relief, **vented deflagration** occurs**. Confined deflagration** differs from the vented deflagration by the absence of significant openings leading to the atmosphere, preventing pressure relief in the enclosure (the peak pressure in a closed vessel for an H_2-air mixture, initially at NTP, can reach a pressure of 815 kPa; (Baker et al., 1983) that would destroy any civil structure generally able to withstand overpressures of about 10-20 kPa).

Deflagration can result in some circumstances in a transition to **detonation**, which differs from deflagration in that there is a leading shock wave, which is coupled with the combustion wave. Due to the higher flame propagation velocity and higher pressures detonations tend to present greater hazards compared to deflagrations.

Both deflagration and detonation present **life safety** hazard through the pressure and thermal effects. They also present **structural explosion safety** hazard, potentially leading to the enclosure collapse. Finally, both delayed ignition events mentioned above can lead to the establishment of **jet fire**, including **fire impinging** on the wall and/or ceiling of the enclosure. Once the jet fire become established, it can occur in either well-ventilated, or in under-ventilated regime, and the subsequent chain of phenomena and safety consequences would follow the pattern depicted in **immediate ignition** branch of the diagram in Figure 1, as illustrated by arrow in a circle pictograms.

2.1.3 Hydrogen safety engineering

It is essential to consider the hazards associated with the design of the system or infrastructure which would involve indoor utilization of hydrogen, preferably at the design stage. A structured approach to this is presented in Hydrogen Safety Engineering (H2SE) which is defined as the application of scientific and engineering principles to the protection of life, property and environment from adverse effects of incident/accidents involving hydrogen (Saffers and Molkov, 2014).

It is paramount to ensure that H2SE is taken into account at the earliest possible stage, preferably during the design of the system or infrastructure which would involve indoor utilization of hydrogen. H2SE involves three main steps or procedures (see Figure 2):

a) Qualitative Design Review (QDR);
b) Quantitative Analysis;
c) Assessment against criteria.

QDR is a qualitative process based on the experience and knowledge of design team. QDR has to be carried out early in the design process and in a systematic way, so that any substantial findings and relevant items can be incorporated in the design of hydrogen application or infrastructure (Saffers and Molkov, 2014).

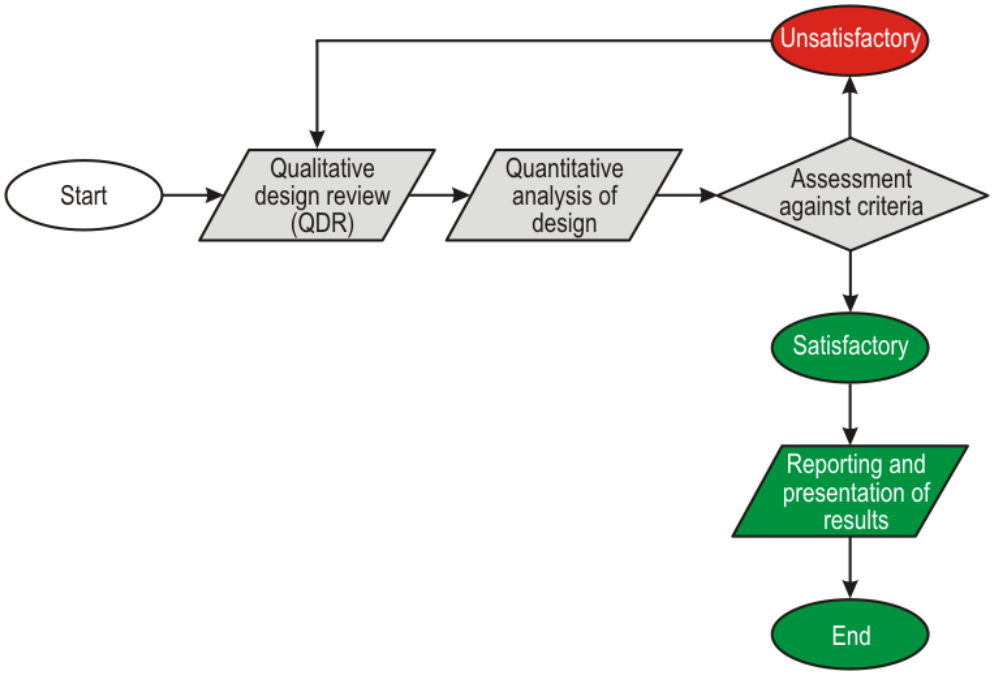

Figure 2. H2SE principles (Saffers and Molkov, 2014).

Quantitative analysis is performed by hydrogen safety expert(s) following the QDR carried out by the team to ensure that the problems are fully understood and that the analysis addresses the relevant aspects of the hydrogen safety system or infrastructure; and to simplify the problem and minimize the calculation effort involved.

Following quantitative analysis, the results should be compared with the acceptance criteria identified by the team during QDR exercise. Three basic types of approach can be considered:

a. Deterministic approach, which shows that on the basis of the initial assumptions a defined set of conditions will not occur;
b. Comparative approach, which shows that the design provides a level of safety equivalent to that in similar systems and/or conforms to pre-existing codes;
c. Probabilistic approach, which shows that the risk of a given event occurring is acceptably low.

2.1.4 General safety rules

General safety rules and strategies of hydrogen infrastructure design include:

- Consider whether it is really necessary to house the hydrogen system within a room / enclosure, or whether it could be positioned outside and therefore subject to better ambient ventilation.
- Minimization of pipeline diameter and operational pressure to satisfy technological requirements to mass flow rate where appropriate;
- Minimization of hydrogen pressure whenever possible;
- Utilization of flow restrictors if decrease of piping diameter is not possible for some reasons;
- Identify, and if possible, separate or eliminate potential ignition sources;
- Utilization of storage tanks allowing to ensure at least sufficient time for evacuation of people in case of fire;
- Minimization of hydrogen inventory, e.g. to exclude formation of flammable mixture even in confined enclosure after complete release and dispersion of hydrogen

2.2 Hydrogen release inside a confined or semi-confined enclosure

2.2.1 Hazards and consequences

Unignited hydrogen release indoors can result in accumulation of hydrogen in the facility. Hazards include:

a) Formation of flammable mixture that potentially could combust if ignited with hazardous pressure and thermal effects.

b) Destruction of enclosure or building by the pressure peaking phenomena during unignited release;

c) Asphyxiation that can result from displacement of breathable air by the hydrogen;

Only the two first events are addressed by Hyindoor project and will be treated in this chapter.

2.2.2 RCS existing information

In most of the standards, not to say all, related to hydrogen, some basic generic requirements are usually mentioned to limit the likelihood of a release, available for indoor or outdoor uses. Examples are:

- Use inherently safe design and technologies,
- Minimize the number of connections,
- limit exposure to hazards through reliability of equipment,
- Apply safety principles when designing control systems…

These means are usually considered as intrinsically safe measures.

With regards to indoor use of hydrogen, some additional general basic requirements are often mentioned to prevent hazards associated with flammable atmosphere accumulations within the enclosure: mainly natural or mechanical ventilation. In some cases additional passive means including pipe orifices or similar methods of flow restriction are mentioned, in order to reduce the accumulation of hydrogen above the lower explosion limit (LEL).

In most cases, a specific risk assessment is required for all stages in the life cycle and all types of potential hazards. The results of the hazard and risk assessment process shall be used both to evaluate the consequences of hazardous events and to determine appropriate risk reduction.

Sometimes specific additional measures and tests are required for specific risk like shock and vibration, for example for mobile applications but not only. It is rarely mentioned that an exhaustive list of hazards or, even better, a standard fault-tree analysis or bow-tie diagram dedicated to outdoor or indoor use of hydrogen needs to be considered.

Part of the requirements remains qualitative without referencing engineering tools, models or methodology. Sometimes, references are made to more specific detailed standards.

With regards to confined spaces, ventilation is generally mentioned as a main requirement in order not to reach a concentration above 25 or 50% of the lower flammability limit (LFL). Reference is made to normal, nominal, foreseeable, abnormal or accidental or other kinds of releases without anymore precision or detailed definition. It also should be noted that, in some standards, hydrogen purges are clearly mentioned as having to be taken into account (for example for fuel cell systems).
In most of the standards, reference is made to standard IEC 60079-10-1 for determining the extent of the flammable region at the source of the release and within the confined area. This standard is a harmonized standard with European so-called ATEX Directive for the prevention of the formation of explosive atmospheres. This IEC standard is not dedicated to hydrogen. It is intended to be applied where there may be a risk of ignition due to the presence of flammable gas or vapor of all kinds (for example methane, gasoline vapors, acetone, hydrogen…) mixed with air under normal atmospheric conditions. As being applicable to different kinds of gases, the generic method described in the standard does not take into account the specific characteristics of a hydrogen release (density, buoyancy, stratification…) and generally

overestimates the concentration in the confined space. There are usually no engineering models, or other methods, mentioned in standards for assessing the hydrogen concentration within an enclosure.

In this IEC standard, it is clearly stated that the catastrophic failures which are beyond the concept of abnormality dealt with in this standard does not have to be considered for the so-called ATEX zoning (for example to the rupture of a process vessel or pipeline or events that are not predictable). But the likelihood of such catastrophic events is limited by appropriate design defined in the existing pressure equipment and piping regulation, standards, codes and practices.

Within existing standards, it is also admitted that the boundary for dilution of normal internal releases to below 25% (LFL) may be verified by computational fluid dynamic analysis, tracer gas, or similar methods, such as those given in IEC 60079-10.

For natural ventilation, openings and ducts are usually mentioned without any detailed information for determining the sizing of these openings. It is also usually mentioned that these openings shall not become obstructed or compromised when the system is normally operated. In some cases, requirement for openings in an enclosure can be contradictory with other requirements on protection from access to hazardous parts complying with a minimum IPXXB or IP2X minimum rating as outlined in Degrees of Protection Provided by Enclosures (IP Code), IEC 60529, including ingress of water.

Gas detection within the confined space is mentioned as possible mitigation measure within most of the standards. If gas detection is employed as a critical safety component, the gas detection system shall usually comply with IEC 60079-29-1 and ISO 26142. The IEC Standard 60079-29-1 specifies general requirements for construction, testing and performance, and describes the test methods that apply to portable, transportable and fixed apparatus for the detection and measurement of flammable gas or vapor concentrations with air.

Usually the detection is intended to trigger the appropriate action determined by the risk assessment of the system, including the prompt shutdown of the equipment or the stating up and monitoring of the ventilation equipment (like fan, blowers…). Failure of ventilation shall cause the system to respond in such a way that shall mitigate any hazard or prevent the creation of additional hazards in accordance with the Safety/Hazard Analysis. This may include shutting off; either through the detection of high gas/vapor concentration or with ventilation interlocks provisions.

In summary, results from Hyindoor will bring valuable inputs for improving guidelines & RCS recommendations and filling some existing gaps in current guidelines and standards as:

- Recommending to use in a proper way flow restrictions in order to limit the maximum flow rate in case of hydrogen leaks;
- Giving General qualitative/quantitative requirements for designing the openings for natural ventilation;
- Proposing validated engineering tools and models for assessing hazard related to hydrogen accumulation within an enclosure, with some different standards configuration of openings;
- Proposing practical nomograms based on these engineering tools and models;
- Proposing a generic phenomena and consequences diagram.

2.2.3 Main outcomes from Hyindoor project on releases in confined space

2.2.3.1 Hydrogen build-up

- **Release characteristics**

- Experiments showed that chocked releases induce more homogeneous build-up regime inside the enclosure compared to sub-sonic releases.
- Concerning the releasing jet, improvement of entrainment modelling is of high importance to predict concentration decay for plumes and/or for plumes/jets at small distance from injection. The knowledge of a reasonable conservative entrainment coefficient would allow the prediction of

maximum concentration (sometimes overestimated by a factor 2) to be improved – Study is still in progress

- CFD showed that moving the source position upward, the concentration:
  - tends to decrease in all regions of the facility for one-opening enclosure
  - decreases in the lower and middle region of the facility while it increases in the upper region for closed enclosure

▪ **Vent configuration**

- Whatever the ventilation mode, increasing the opening area enhances the ventilation, limiting hydrogen build-up; it can be obtained:
  - By increasing the size of the vents,
  - And/or by increasing the number of vents.
- For equivalent ventilation area, a two-openings configuration (vents at top and bottom of the enclosure) is more efficient than a one-opening configuration (vents only at top of the enclosure).
- The larger height difference between multiple vents is, the more efficient is passive/natural ventilation.
- Comparison of the ventilation efficiency between vents of the same area located on the vertical wall and on the horizontal roof (but protected by a chimney with a cover to avoid rain and snow entering) clearly indicates that wall vents are more efficient and that external protection decreases the ventilation efficiency.
- CFD simulations showed that the connection of a duct or adding a rain cover just outside the vent decrease natural/passive ventilation efficiency.
- CFD simulations showed that vertically stretched vents (height > width) provide better ventilation compared to horizontally stretched vents of the same area.

▪ **Wind effects**

- Experiments showed that it is difficult to determine a characteristic wind for a specific site due to the variability of this uncontrollable environmental parameter (velocity, orientation...)
- Several vents distributed on all sides of the enclosure (both at the top and the bottom) help to ensure that wind would enhance ventilation regardless of its direction.

2.2.3.2 Pressure peaking phenomenon

Pressure peaking is the phenomenon observed for very lighter than air gases, which can result in overpressure exceeding enclosure or building structural strength limit in case of sufficiently high hydrogen release rate. In order for pressure peaking to occur, the hydrogen release flow rate should be sufficiently high to result in complete displacement of air from the enclosure, i.e., hydrogen concentration within enclosure must reach 100%.

This phenomenon was theoretically and experimentally treated in Hyindoor project. The main are the following:

- Pressure peaking effects on the structure of an enclosure were experimentally observed to confirmed analytical developments
- PPP observation is finally a complex combination of the following parameters:
  - High release flow rate,
  - Small enclosure,
  - Small size of vents;

- Calculation of vent sizing should take into account possibility of pressure peaking phenomenon (PPP). An example of graphical tool (nomogram) which provides estimation if 100% hydrogen concentration will be reached for a given release rate and vent dimensions is provided in Appendix 4.2.1.1 (Molkov et al., 2014).
- Experimental measurements of maximum overpressure due to PPP were compared against theoretical model (Brennan and Molkov, 2013). The theoretical model fits quite well to experimental data with the difference that it gives overestimated values at higher hydrogen flow rates compared to the experiments
- If 100% hydrogen concentration is achieved, the estimate of resulting overpressure due to PPP can be obtained using analytical and graphical tools, such as nomogram provided in Appendix 4.2.1.2.
- If vent area is fixed, a way of preventing structural damage due to PPP is to reduce the hydrogen release rate through reduction of the tubing diameter.
- In case of hydrogen jet-fire the PPP can occur with even more dangerous due to release of large quantity of light hot gas, the level of overpressure can be evaluated by the “rule of thumb” presented in Appendix 4.2.1.4.
- Maximum over-pressure due to PPP is practically independent of vent location

2.2.4 Consequences assessment: Analytical and numerical approaches

2.2.4.1 Build-up consequences assessment

2.2.4.1.1 Simple approaches for build-up consequences assessment

- **One-opening modelling approach**

One-opening ventilation mode is obtained by adding opening at the top of the considered enclosure.

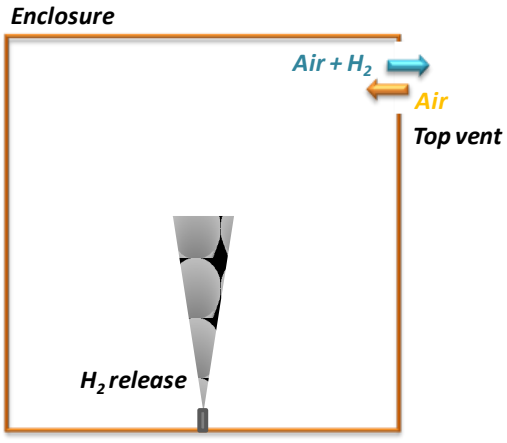

Figure 3. One-opening ventilation mode

Enclosure can be equipped with one or several apertures, but when apertures are multiple they are all:

- at the top of the enclosure,
- at the same altitude,
- identical, i.e. with the same shape and the same height (not necessarily the same length).

Two analytical modelling approaches were tested and validated:

- The passive ventilation proposed by Molkov et al. (2014),
- The natural ventilation presented first by Linden (1999) and slightly modified by Cariteau and Tkatschenko (2013).

- Appendix 4.2.2.1 provides equations and the nomogram for calculation of sizes (height and width) of a single vent in case of uniform mixture in the enclosure with a single vent (Molkov et al., 2014). Note, that although in practice hydrogen-air mixture can form layers even in the enclosure with one vent, equations and the nomogram in Appendix 4.2.2.1 will provide results close to the maximum concentration values, i.e., it is conservative and can be applied to non-uniform mixtures.
- Linden model (1999) can be used too through the simplified expression proposed by Cariteau and Tkatschenko with a discharge coefficient of 0.25 (see Appendix 4.2.2.2).

Forced ventilation should be applied in cases when passive ventilation is impractical or insufficient, e.g. because it would require too large vent area to ensure the hydrogen concentration remaining below LFL, etc. Considering one-opening ventilation mode with uniform mixture, the Molkov et al. approach (2014) can also be used to design forced ventilation.

Waiting further advancement on this topic, a methodology is presented in Appendix 4.2.2.3 to determine needed extracting or blowing forced flow rate for a targeted hydrogen build-up concentration.

- **Two-openings modelling approach**

Ventilation system with two vents is more effective than a system with one vent of the same area.

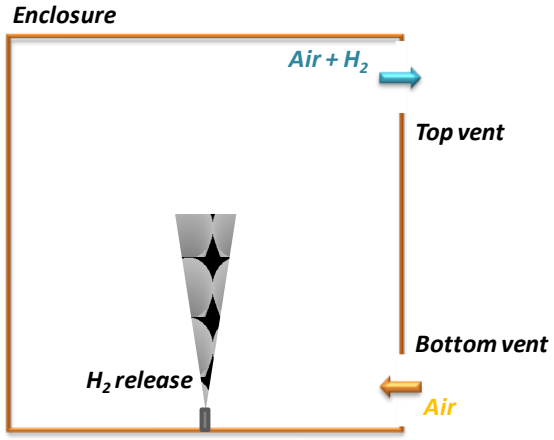

Figure 4. Two-openings ventilation mode

Two-openings ventilation mode is obtained by adding openings located at the top and at the bottom of the considered enclosure. Openings must have a difference of altitude.

Multiple-vents system should be used for ventilation, but for openings at the top as for the openings at the bottom, they should follow the following characteristics:

- the same shape and the same height (not necessarily the same length).

- The Linden modelling approach (1999) can be used as simple engineering model for the two-openings ventilation mode (see Appendix 4.2.3).
- Presently, there is no engineering correlation for complex openings ventilation systems like distributed multi-vents configurations.

- **Wind consideration**

- Analytical models like Molkov et al. (2014) and Linden (1999) do not take into account wind, but these models remain conservative in most of the cases regarding the calculated concentrations inside a semi-confined enclosure.

- Effect of wind especially with changing direction should be studied in future in more detail to be able to formulate engineering tools for hydrogen safety engineering.

2.2.4.1.2 CFD: best practices and limits of use for build-up assessment

- LES CFD approach is the numerical modelling which gives the more accurate results, but flow rates conditions remain unclear; probably more adapted for plume releases
- Laminar CFD approach allows fast calculation but seems not really accurate
- RANS k-epsilon CFD approach
  - is not adapted for low release flow rates
  - is not conservative for high releases flow rates
- CFD models could be applied for complex openings configuration (for instance multiple-vents) if they pass verification against experiments.

2.2.4.2 Pressure peaking consequences assessment

- If 100% hydrogen concentration is achieved, the estimate of resulting overpressure due to PPP can be obtained using analytical and graphical tools, such as nomogram provided in Appendix 4.2.1.2
- Maximum PPP overpressure could be also calculated using the theoretical model (Brennan and Molkov, 2013)

2.2.5 Recommendations for risk assessment and RCS

Design

- In order to prevent accumulation of flammable concentrations of hydrogen an enclosure should be provided with adequate passive vent(s). If practical, ventilation system should be designed to prevent concentrations exceeding LFL for realistic expected hydrogen release rates.
- Utilization of two (or more) vents located at different height is preferable; this ventilation configuration is more effective than a single vent (or more) only located at the top of the enclosure, considering the same total ventilation area.
- A one-opening ventilation configuration can be used when a two-openings ventilation configuration is not possible;
- Vents on vertical side walls of the enclosure are preferable to horizontal roof vents;
- Obstructions – like grids or ducts in front of the ventilation vents should be avoided. When it is not possible (e.g., due to thermal or security reasons), account should be taken for the reduction of the ventilation performance. The effective ventilation area has to be re-calculated and a correction factor addressing efficiency reduction should be introduced in order to take into account the reduction of the discharge coefficient due to vent obstruction;
- Forced venting could be applied in cases when purely passive ventilation is impractical, e.g. since it requires too large vents unacceptable at cold climate. It should be recognised, however, that such systems are not necessarily fail-safe and the reliability of the forced ventilation system needs to be considered;
- PPP has to be taken into account in risk assessment.

Calculation means for build-up assessment and ventilation system sizing

- Ventilation system parameters can be calculated using engineering tools described in Appendix 4.2:
  - For one-opening ventilation mode
    - The passive ventilation approach proposed by Molkov et al. (2014)
      - By using equations
      - By using proposed nomograms
    - The natural ventilation approach proposed by Linden (1999); the simple expression developed by Cariteau and Tkatschenko (2013) is validated and usable (see Appendix 4.2.2.2)
  - For two-openings ventilation mode
    - The natural ventilation approach proposed by Linden (1999) (see Appendix 4.2.3)
- Waiting new developments, forced ventilation in an enclosure with one opening could be calculated using equations proposed in Appendix 4.2.2.3.
- Computational Fluid Dynamics (CFD) can be an interesting approach especially for complex geometries, multiple vents and release parameters different from those more classical considered to develop analytical engineering tools.
- PPP can be assessed using Brennan and Molkov (2013) theoretical model, or using the experimental correlation proposed in Appendix 4.2.1.2

2.3 Indoor hydrogen-air deflagration

2.3.1 Hazards and consequences

When it is not possible to avoid a hydrogen-air mixture with a hydrogen concentration lower than LFL (i.e. more than 4%), the ignition of this flammable atmosphere can occur and induce dangerous consequences due to its combustion.

Thus the following events can be considered:

- Hazardous pressure effects of deflagration:
  - Overpressure: typical pressure to destroy civil structure is 10-20 kPa;
  - Impulse: provides projectiles in case of enclosure demolition.
- Hazardous thermal effects:
  - Direct engulfment of people into hot combustion products of deflagration (volume of combustion products is E_i times larger compared to volume of initial flammable mixture, where E_i is expansion coefficient of hydrogen-air mixture combustion);
  - Radiative heat flux to humans and equipment from combustion products.

Hyindoor works are focused on vented deflagration phenomenon; results and recommendation concerning this topic are presented in the following sections.
Deflagration is the ignition and the combustion of a flammable mixture (here hydrogen-air) in a confined space which will generate internal overpressure leading in some cases to enclosure destruction. The presence of vents, depending on their characteristics, will allow the internal overpressure to be decreased. Thus these vents are a mean to mitigate the consequences of an explosion.
For this event, the dispersion inside the enclosure is considered established that is why it can be referred as delayed ignition phenomenon.

2.3.2 RCS existing information

In addition to mitigation measures prescribed in the previous chapter for preventing releases or accumulation, additional generic mitigation measures are required in most standards to avoid or limit consequences of explosion outdoor or in an enclosure.

The first set of measures is intended to prevent ignition of the confined hydrogen cloud, by eliminating the potential ignition sources using some of the following means:

- Proper grounding and bonding of metallic parts;
- Selected materials that do not generate charges that could result in a spark capable to ignite a flammable gas/air mixture. The effect of flow rates within pipes generating possible charges shall be considered too;
- Install electrical equipment suitable for the area classification according to IEC 60079-0* and other applicable parts of the IEC 60079 series;
- Surface temperatures not exceeding 80% of the auto-ignition temperature;
- Equipment containing materials capable of catalyzing the reaction of flammable fluids with air capable of suppressing the propagation of the reaction from the equipment to the surrounding flammable atmosphere.

In most standards, requirements are given on floor, walls and ceiling of enclosures for example for construction materials, height & design, fire-resistance rating, openings and doors. Sometimes, it is added that all the walls, doors, roofs not intended for explosion relief shall be designed to contain deflagration. But there are a few mentions to vented explosion and vent covers. The requirements then consist in general qualitative requirements and examples as:

- Walls of light material;
- Lightly fastened hatch covers;
- Lightly fastened, outward-opening, swinging doors in exterior walls;
- Lightly fastened walls or roofs.

Practical important information is sometimes added such as considering potential snow loads for example. There are no quantitative requirements or references to engineering models and tools to assess consequences of a vented explosion and/or size proper vents or covers in existing standards.

Even if venting deflagrations is the most wide spread technique to mitigate explosions in an enclosure, there is also no international reference standard related to explosion venting protection system for hydrogen application. There is a European standard, EN 14994-Gas explosion venting protective systems, that specifies the basic design requirements for the selection of a gas explosion venting protective system but it is not applicable to hydrogen explosion. In US, NFPA 68 is the only national standard dealing with the inertial vent covers for hydrogen.

In summary, results from Hyindoor will bring valuable inputs for improving guidelines and RCS recommendations by:

- Proposing validated models for assessing more accurately over-pressure in vented explosion;
- Defining the appropriate vents size to ensure not exceeding a maximal targeted overpressure allowing as much as possible the structure destruction to be avoided. Or if not possible, by setting up a dedicated safety strategy to reduce the likelihood of such an event or implementing corresponding safety distances.

2.3.3 Main outcomes from Hyindoor project on indoor deflagration phenomena

- Ignition of flammable hydrogen-air mixture at central part of enclosure or at a rear wall typically leads to a higher maximum deflagration overpressure compared to a near-vent ignition;
- Delayed ignition of hydrogen jets and releases forming localised highly turbulent hydrogen-air cloud may lead to significant overpressure in ignition vicinity even though average concentration in vessel may be low (e.g. ~1% v/v);
- Vented deflagration of a stratified hydrogen-air mixture may lead to significantly higher overpressure compared to the lean uniform hydrogen-air composition with the same hydrogen inventory.
- Congestion (i.e. high blockage ratio) inside the enclosure accelerates flame and causes higher deflagration overpressures;
- The deflagration overpressure decreases when the vent surfaces are increased;
- The larger the vent area, the higher the concentration of the flammable mixture can be without destroying the enclosure;
- Effectiveness of deflagration venting is not affected by vent orientation (horizontal or vertical);
- A single vent of larger area or multiple vents will suppress flame acceleration and higher deflagration overpressures.

2.3.4 Consequences assessment: Analytical and numerical approaches

2.3.4.1 Vented deflagration assessment

2.3.4.1.1 Simple approaches for vented deflagration consequences assessment

- 1999 and 2013 Molkov approaches could be used to predict deflagration over-pressures for lean mixtures; these models are conservative;
- FM Global analytical approach was calibrated and validated for stratified dispersion configurations on Hyindoor experiments. A further development is needed to integrate this result in the modelling approach.

2.3.4.1.2 CFD: best practices and limits of use for vented deflagration consequences assessment

- Computational Fluid Dynamics (CFD) can be used for complex geometries, multiple vents and parameters which cannot be described by classical analytical engineering tools;
- CFD models are capable to reproduce major experimentally observed deflagration dynamics features;
- Care should be taken to ensure that CFD models are validated for the same range of parameters for which they are applied: hydrogen concentrations, enclosure scales, congestion, vent size, etc.

2.3.4.2 Hydrogen inventory limitation preventing enclosure destruction

A thermodynamic model may be used to predict maximum mass of hydrogen, which is allowed to be released in an enclosure without causing destructive overpressure in case of its combustion. The model presumes that localised hydrogen-air mixture fills enclosure only partially and burns in a completely sealed enclosure. To limit maximum overpressure from deflagration of such a localised mixture in a closed volume by 10 kPa, the model solution for hydrogen mass is $m_{H2} < 2.61 \cdot 10^{-4} V$, where m_{H2} is mass of hydrogen (kg), V is enclosure volume (m^3). Model methodology is described in Appendix 4.3.1.

Note that local damage may still occur to the structure if a layer of higher hydrogen concentration forms within the room/enclosure and detonation occurs, such as in areas of high congestion (Friedrich et al, 2007).

2.3.5 Recommendations for risk assessment and RCS

Design

- Venting of deflagrations is the most widespread technique to mitigate explosions in an enclosure decreasing overpressure;
- Apertures initially dedicated to ventilation will participate in the venting of the explosion;
- The size of the vents should be chosen to ensure that overpressure produced by mixture deflagration will not exceed structural strength of the enclosure;
- Internal overpressure in case of ignition decreases with increase of vent surface(s);
- Position potential ignition sources close to explosion relief vent if possible;
- When possible prefer vents dedicated to natural/passive ventilation without obstruction (or minimizing obstruction: grids for instance) to limit overpressure in case of deflagration;
- Avoid or minimize internal congestion in the enclosure;
- The gases vented from a deflagration need to be discharged into a safe area.

Calculation means for overpressure assessment and vents sizing

- State-of-the art correlation for vent sizing for a low strength equipment and buildings (deflagration overpressure below 1 bar) developed within the HyIndoor project is presented in Appendix 4.3.2.
- Vent size can be calculated using analytically derived and experimentally validated correlations between allowable overpressure, enclosure volume, flammable mixture parameters, and vent area. Appendix 4.3.2 presents a correlation for the case of hydrogen fraction uniform across the entire enclosure (Chernyavsky et al., 2014). Appendix 4.3.3 presents a technique to calculate vent size for the case when hydrogen-air mixture occupies only part of the enclosure volume, i.e. a layer with uniform and non-uniform concentration.
- CFD may be used to predict vented deflagration pressure dynamics, particularly - where simplified engineering models are not applicable.
- However, care should be taken to ensure that CFD models are validated within range of parameters for which they are applied, including:
    - hydrogen concentration
    - enclosure scale
    - internal congestion
    - vent size
    - vent inertia

2.4 Dealing with hydrogen jet fire and underventilated fire

2.4.1 RCS existing information

Unlike the previous sections, while standards mainly cover leaks and how to avoid them, and somewhat cover how to avoid or limit consequences of explosions outdoor or in an enclosure, existing standards do not cover underventilated jet fire except for some general recommendations to protect goods or people as safety distances for example. But this is not specifically related to indoor use.

2.4.2 Main trends from numerical and experimental studies

From numerical studies and 1 m^3 scale experiments it was concluded that as a general rule the increase of hydrogen flow rate changes the fire regime in the enclosure with one upper vent from the well-ventilated fire, through transition of internal combustion to the external flame at moderate flow rates, and to the complete self-extinction of combustion in the whole domain at higher flow rates. Thus, two modes of under-ventilated fire are observed in this numerical study. One mode is the external flame, and another is the self-extinction of flame. The reason behind the observed transition between these two regimes is more intensive cooling of combustion products within the enclosure for higher release rates. In both modes, unburnt hydrogen accumulates within the enclosure. At the 31 m^3 experimental scale, with the release point some 3.5 m from the open vent, no external flame was observed, even during under-ventilated tests, presumably due to there not being the coincident existence of sufficient hydrogen, oxygen or temperature. This does not imply that external flames could not occur under different conditions.

The general rule for indoor fire with one lower vent is formulated, i.e. an increase of hydrogen release flow rate changes fire regime from: well-ventilated fire (small leak rates), to under-ventilated fire with self-extinction of combustion and again to under-ventilated fire with external flame.

The following should be noted: Flame extinguishes at a lower leak rate than comparable upper vent case. No external flame mode observed between well ventilated mode and extinguishment mode. Ghosting flames were observed. Transition from extinguishment to external flame regime occurs at lower leak rate than upper vent case. No harm distance based on temperature is greater for the same leak in upper vent scenario where vent size and release rate is comparable.

In the case with two vents of the same area (one upper and one lower) general rule is: an increase of a hydrogen sustained release flow rate will change the fire regime from well-ventilated combustion within the enclosure through to the “micro” combustion and then to an external flame scenario. Thus, two modes of under-ventilated fire are observed in this numerical study. One mode is the external flame, and another is the “micro” combustion of flame.

For the self-extinction regime the one way flow through the enclosure vent is observed. This terminates conditions when undiluted hydrogen and air are available in sufficient amount in the vicinity of existing flame (acting as "ignition source") and finally ceases combustion.

At the 30 m^3 experimental scale in under-ventilated conditions, hydrogen accumulation was observed even when the measured oxygen concentration in the enclosure was relatively high, 8 – 15% v/v. No hydrogen accumulation was observed under well-ventilated conditions, when the measured oxygen concentration remained greater than 18% v/v.

The main hazards and consequences:

- Hot temperature in fire and jet of combustion products. Temperature in a jet fire hot current decays to “no harm” value of 70^{o}C at distance from the release 3.5 times longer than jet flame itself. Pain separation distance (deterministic) is 3 times of the jet flame length. Fatalities can happen at distance twice as long as flame length. It should be underlined that all three deterministic separation distances from well-ventilated jet fires are equal or longer than distance to LFL in case of unignited release from the same source (Molkov, 2012);
- Thermal radiation from surfaces heated by impinging fire and from hot layer formed during a fire under the ceiling. Harm criteria from radiation can be found in Appendix 4.1.1. Thermal radiation can affect evacuation of people from a site;
- Hydrogen accumulation, and subsequent internal explosion, resulting from under-ventilated jet-fires.
- Pressure effects of jet fires indoors. Pressure peaking phenomenon for jet fires is more pronounced compared to pressure peaking during unignited release from the same source.
- Oxygen depletion that could cause asphyxiation.
- Secondary fires with toxic combustion products.

2.4.3 Phenomenon modelling approaches

Hydrogen subsonic ignited releases into 1x1x1 m^3 enclosure were modelled; Different vent configuration were used i.e. one upper (vertical or horizontal), one lower, and two vents (upper and lower); Pipe diameters applied: 5.08 mm and 20 mm, velocity range 15-1100 $m.s^{-1}$.

Tested modelling approach:

- The Reynolds averaged Navier-Stokes (RANS) computational fluid dynamics (CFD) model
- The model is based on the renormalization group (RNG) k-ε turbulence model (Yakhot and Orszag)
- The eddy dissipation concept (EDC) model by Magnussen for simulation of combustion
- The 18-step reduced chemical reaction mechanism of hydrogen combustion in air with 8 species (subset of the Peters and Rogg's mechanism that excludes H_2O_2 formation and consumption
- The in-situ adaptive tabulation (ISAT) algorithm by Pope that accelerates the chemistry calculations by two to three orders of magnitude

Range of application of modelling approach:
Model capable to reproduce all indoor regimes: well-ventilated, under-ventilated (self-extinction and external flame modes) along with oscillations and ghosting flames. The heat transfer through the walls has been also accounted.

The main modelling features: condensation and radiation are not considered; mesh resolution across vent to resolve at least by 12 CVs to allow two way flows across the vent. The use of the external computational domain is essential to provide adequate air movement from the far boundary to the vent.

CFD modelling, of the well-ventilated experiments in the all-metal 30 m^3 enclosure was able to provide reasonable predictions of the internal temperatures when the thermal boundary conditions at the walls were approximated by using the isothermal outdoor temperature. Fires within enclosures with more insulating walls, such as brick, would require a more sophisticated approach.
Results of experiments have been qualitatively reproduced.
CFD can successfully be used as a design tool for hydrogen safety engineering.

2.4.4 Recommendations for risk assessment and RCS

Design

- Where practicable, avoid the conditions for under-ventilated jet-fires to occur by providing sufficient ventilation. This may be achieved by providing sufficient passive vents to maintain an average concentration of less than the LFL resulting from an unignited hydrogen leak.
- Use fire resistant materials where possible;
- Avoid the presence of combustible materials close to vents if there is a potential for an underventilated jet-fire to occur.
- Consider protection against under-pressure due to rapid steam condensation (e.g. by providing vents for emergency air inflow or inert gas injection).

Calculation means

- Appendix 4.4.1 presents the dimensionless correlation for calculation of flame length (Molkov and Saffers, 2013). Results of the flame length calculation can be used to find out three deterministic separation distances for well-ventilated jet fires. An example of the tool for calculation of deterministic separation distance is provided in Appendix 4.4.3;
- Use piping of smallest possible diameter or introduce flow restrictors to reduce flame length (flame length is generally proportional to leak diameter). An example of calculation of the effect of flow restrictor on flame length is provided in Appendix 4.4.2;

- Radiation heat flux from the hot layer of combustion products and heated ceiling can affect the evacuation. The methodology to calculate thermal radiation and example based on HSL experiment are given in Appendix 4.4.4;
- Computational fluid dynamics (CFD) can be used as a contemporary tool for hydrogen safety engineering in assessment of jet fires indoors as no other tool available.

2.5 Safety means or strategies to limit consequences

Industrial designers/users have to choose adequate safety strategies regarding the application and its environment. Based on this analysis, they have to determine safety objectives that they will have to respect considering several failure scenarios.

2.5.1 Limiting hydrogen build-up in confined space

2.5.1.1 General means for design

- Respect as much as possible the recommendations presented in section 2.2.5 p 18
- If safety objectives are based on hydrogen concentration build-up inside the enclosure, and are not achieved, it is possible to investigate the following mitigation means:
    - The forced or mechanical ventilation which allow releasing hydrogen to be evacuated
    - The flow restrictors can be installed at strategic location in piping to limit release flow rate in case of full bore rupture, thus limiting hydrogen build-up
    - The detection devices can early alert operators in case of release before reaching LFL and launch automatically safety actions

2.5.1.2 Mechanical ventilation

Forced ventilation can be an efficient mitigation mean. However choice and design of a ventilation pattern is complex. Some characteristics which must be considered are given below:

- Operating conditions:
    - blowing or extraction, if extraction is chosen the equipment must be ATEX-certified
    - Automatic or manual
    - Permanent or occasional (on-demand)
    - Ventilation flow rate
- Setup:
    - Sufficient openings for air admission or expulsion (according to the ventilation mode)
    - Correct location of openings in order to avoid by-pass (i.e. areas which will not be ventilated)
    - Take car about congestion which can create unventilated areas too

2.5.1.3 Flow restrictors

In the cases where a predictable flow rate value is known to be too large to achieve desired safety objectives, flow restrictors could be used to reduce the maximal leakage flow rate. A correlation is given in Appendix 4.4.2.

2.5.1.4 Detection

Hydrogen sensors are risk mitigation devices allowing for the detection of a potentially explosive atmosphere arising from unwanted release of hydrogen (leaks) which subsequently mixes with air. For their deployment, often questions arise as to which sensor type to use, how many sensors to use and where to place them. For optimal deployment of hydrogen sensors both the requirements for the specific application and the sensor performance need to be taken into account. Hydrogen sensors should be integrated into a general safety strategy, which is strongly dependent on the specific application.

In these guidelines some general recommendations for the choice and placement of sensors are given, followed by considerations for a few specific applications.

Locally applicable legal requirements can be found in the relevant standards and regulations (for example ATEX 137, IEC 61779, IEC EN 60079, NFPA 70). Identification of potential hazards due to use of hydrogen can be achieved using any of several established industry methods, such as FMEA (Failure Modes and Effects Analysis) [Safety Planning Guidance for Hydrogen and Fuel Cell Projects, 2010]. Accordingly, a risk reduction plan may include the placement of a gas detection system.

2.5.1.4.1 Types of hydrogen sensors

There are a large number of hydrogen sensors available for purchase on the market and these sensors commonly employ one of the following detection technologies (for an overview refer to Hübert et al. (2011)):

1. **Thermal conductivity (TCD)**. TCD sensors exploit the exceptionally high thermal conductivity of hydrogen gas, which is approximately 7 times higher than that of air. The hydrogen concentration is inferred from the rate at which a sensing thermal element releases heat compared to a reference element. Being based on a physical effect, no catalytic materials are needed; thus, this sensor platform shows high lifetime and resistance to poisoning.

2. **Catalytic (CAT).** This platform is based on the reaction of a combustible gas (such as H_2) and O_2 which happen at the catalytic surface of the sensing point. The reaction generates heat which determines a change of the resistance of the sensing element, usually a ceramic bead (pellistor). This platform is a well-developed and commercialised technology typically used for detecting combustible gasses up to the LFL.

3. **Electrochemical (EC).** This general class of sensors includes amperometric, potentiometric, and solid/liquid electrolyte type sensors. EC gas sensors relate the target gas concentration to the change in an electrical parameter due to electrochemical reactions occurring at the sensing electrode. EC sensors are one of the most widely available commercial sensor platforms, especially amperometric sensors, due to their linearity and repeatability over a broad range.

4. **Metal-oxide sensors (MOx).** MOx hydrogen sensors are widely available on the market and are popular due to their low cost and ease of use. The active sensing material is a semi-conducting metal-oxide such as tin oxide. The electrical resistance of metal oxides decreases at elevated temperatures relative to its resistance at room temperature. The resistance of the active material also changes in the presence of reducing gases such as hydrogen. Despite their low cost and their high sensitivity, MOx sensors can become saturated at modest hydrogen concentrations and exhibit poor selectivity to hydrogen, responding to other reducing gases such as carbon monoxide, methane and water vapour (Boon-Brett, 2009).

5. **Metal-oxide-semiconductor (MOS).** This sensor type is characterized by a three layer structure: a catalytic metal layer, an oxide layer and a semiconductor substrate. Hydrogen atoms form a dipole layer at the metal/oxide interface, which causes a change in the work function (i.e. the minimum energy required to remove an electron from a solid surface) of the metal that is proportional to the hydrogen concentration. The change in work function can be measured using Schottky diodes, capacitors or field effect transistors.

6. **Resistance-based Palladium thin film (PTF).** PTF sensors are based on a change of electrical resistance of a thin film of palladium following absorption of hydrogen. Hydrogen molecules are split at the Pd surface and atomic hydrogen is absorbed into the metal lattice forming palladium hydride which has a higher resistivity compared to palladium. Commercial PTF sensors show good performances but may incur high costs.

In addition there are devices which employ more than one technology to detect the presence of and quantify the concentration of hydrogen.

2.5.1.4.2 Good practices for an efficient use of detection

- **Placement and number of the sensors in a confined space**

The two basic approaches to the location of gas detectors are (Jessel, 2002):
1. **Point source monitoring**, where the sensor is sited close to an identified potential leakage point, such as such as valve stem seals, gaskets, compression fittings and expansion joints;

2. **Perimeter or area monitoring** for extensive areas, where a plant or process is ringed by monitors or a network of sensors is deployed to give early warning of a leak but no specific location of the leak is identified.

As hydrogen is lighter than air, it will move to and diffuse along the ceiling and will tend to escape through any openings present. The exact path of the gas or its dispersion characteristics will depend on the density of the gas and the ventilation patterns. The following considerations assume a minor leak scenario. Other transport mechanisms than diffusion are active for large leaks (hydrogen jets), in which case a more complex approach for determining sensor placement is advisable, such as CFD modelling.

For optimal placement of a sensor, the dimensions and configuration of the volume to be monitored, gas dispersion and ventilation patterns need to be considered

Thus, some general instructions can be given:

- The position of the sensor should be on or close to the ceiling, especially in areas where gas build-up is likely to happen, such as corners or stopping points of gas-releasing moving devices
- If possible, the position of the sensor should be placed just above possible sources of leak, such as valves and gaskets. However, nuisance alarms can be avoided by not placing the sensor too close to equipment that may have minor leakage in normal operation.
- Attention should be given to ventilation patterns, because the performance of hydrogen sensors may have marked flow dependence
- Consideration of openings in the enclosure (doors, windows...); these openings can decrease the hydrogen concentration locally, therefore the sensor must be sufficiently sensitive
- In case a point leak source cannot be identified, a grid of hydrogen sensors may be placed on the ceiling
- Areas not reached by the ventilation system need to be monitored by additional sensors
- The sensors should not be positioned in areas where they may be susceptible to damage through vibration, heat, contamination or water damage
- The sensor orientation will be specified by the manufacturer. Typically they should preferably face down towards the area where the leak is expected. This position would also avoid the accumulation of dust on the sensing head, which may impede the diffusion of gas into the sensor
- The number and placement of sensors depends on the ventilation as well as the volume of the space and the leak rates to be monitored [Safety Standard for Hydrogen and Hydrogen Systems, 1997]. The area a single sensor can monitor can therefore vary, but could be on the order of around 50 m^2
- CFD modelling could be a promising approach to optimize placement and number of sensors for complex installations (e.g. Heitsch, 2010).

- **Gas detection in hazardous areas**

- A gas sensor for use in hazardous areas needs to be constructed in such a way that it will not provide a source of ignition. It should have the appropriate markings (“CE” and “Ex”) to show conformity with the relevant regulations
- In Europe equipment to be used in a potentially explosive atmosphere is covered by the EC directive 94/9/EC (ATEX Regulations). Hydrogen gas detectors used for safety shall comply with ISO 26142 and IEC 60079-29-1. Selection, installation, use and maintenance of hydrogen gas detectors shall be in accordance with IEC 60079-29-2
- When possible, the control panel should be located so that readings can be taken safely, outside the hazardous area. There should also be convenient access for calibration and maintenance

- **Alarm set points**

- For leak detection purposes it may be practicable to set two alarm levels. Depending on the application, the first alarm level could be set to 10% of the lower flammability limit (LFL, for hydrogen being 4 vol% in air) and the second alarm level at 25% of the LFL.
- The hydrogen sensor needs to be integrated with the general safety system and linked to appropriate measures such as a shut-down of the system. Visual and audible alarms should be provided as necessary. After an alarm has been triggered, persons re-entering an enclosed space should use a portable hydrogen (and oxygen) detector.

- **Maintenance and calibration**

- Sensors should be calibrated before use in order to ensure an accurate response
- The degradation of the sensor will depend on the type and on the operating conditions. These factors will affect the frequency of inspection, maintenance and calibration. Maintenance and calibration intervals recommended by the manufacturer should be respected as the minimum.

Only suitably qualified and trained personnel should carry out calibration and maintenance, as specified by the manufacturer

2.5.2 Limiting effects of explosion in confined space in case of ignition

- Respect as much as possible the recommendations presented in section 2.3.5 p 22
- If safety objectives are based on structure strength following a deflagration, and are not reached, it is possible to investigate the following mitigation means:
    - Adding of dedicated vent panels with optimized kinetic and dynamic of these openings
    - Establishment of safety distances
    - Use of other means to reduce internal overpressure
        - Absorbing materials inside the enclosure could be studied
        - Or other protection systems against internal overpressure...
    - Increase of the structure strength by adding structural reinforcement materials

2.5.3 Limiting effects of underventilated fires

There is a potential danger of re-ignition inside of enclosure where after self-extinction of jet fire the release is keep on going and there is still some materials glowing so this need to be considered carefully.

- Respect as much as possible the recommendations presented in section 2.4.4 p 24

Further works are needed on these phenomena before proposing other efficient ways to avoid associated risk.

3. Conclusions

Deliverable 5.1 makes a summary of the main research results of the Hyindoor project.

A focus is made on undisputable results which have been translated as simple as possible in order to provide usable information for engineers who are involved in design, conception and safely use of indoor hydrogen energy applications.

In a first step of this project a state of the art of the knowledge was performed in order to address the relevant questions to Hyindoor project.

In the same time, a review of existing systems and of critical risk scenarios was carried out to prioritize and choose the research actions to be led in Hyindoor project.

Thus, the four following main topics were identified and treated experimentally, analytically and/or numerically:

- Hydrogen release inside semi-confined enclosure,
- Indoor hydrogen-air deflagration,
- Jet fire and underventilated fire,
- Hydrogen detection for confined spaces.

In conclusion of the work performed in Hyindoor project, research results obtained in each work package were analyzed, criticized and translated in easily understandable and usable general rules and calculation means for consequences and mitigation assessment and/or sizing.

Thus this Guidelines document presents recommendations to integrate safety through the applications.

For the design and for consequences or mitigation effectiveness assessment several calculation means are proposed.

When possible, nomograms were built for easy and quick handling of phenomena consequences assessment.

Simple engineering approaches are proposed as well, and recommendations are given for a correct use of the numerical simulation tools.

To conclude this document, keep in mind that best practices, methods, calculation means presented here are the state of our knowledge at this time and that this knowledge will be improved thanks to our continuous work on safely use of hydrogen energy.

References

Administration (1997), N.A.a.S., Safety Standard for Hydrogen and Hydrogen Systems. NSS 1740.16

APPEA (1998), Australian petroleum production & exploration association limited (APPEA), Guidelines for fire and explosion management (1998).

Baker W.E., Cox P.A., Kulosz J.J., Strehlow R.A. and Westine P.S. (1983), Explosion Hazards and Evaluation, Fundamental Studies in Engg. 5, Elsvier, 1983.

Baker P., Sharpless S., Ward I. (1987), Air flow through cracks, *Building and Environment*, Pergamon 1987, 22(4) : 293-304.

Barry T.F. (2003), Fire exposure profile modelling: some threshold damage limit (TDL) data.

Brennan S. and Molkov V.V. (2013), Safety Assessment of Unignited Hydrogen Discharge from Onboard Storage in Garages with Low Levels of Natural Ventilation, *Intl J. of Hydrogen Energy*, 38 (19): 8159–8166.

Bryan J.L. (1986), Damageability of buildings, contents and personnel from exposure to fire, *Fire Safety Journal*, 11: 15-31.

BSI (1997) British Standard 7899-2:1997. Code of practice for assessment of hazard to life and health from fire. Guidance on methods for the quantification of hazards to life and health and estimation of time to incapacitation and death in fires. British Standards Institution, 1997.

BSI (2004) British Standard Published Document PD 7974-6:2004 (2004), The application of fire safety engineering priciples to fire safety design of buildings. Human factors. Life safety strategies. Occupant evacuation, behaviour and condition (Sub-system 6), British Standards Institute, 2004.

BSI (2007) British Standard BS EN14994:2007, Gas explosion venting protective systems, British Standards Institute, 2007.

Boon-Brett, L., J. Bousek, and P. Moretto (2009), Reliability of commercially available hydrogen sensors for detection of hydrogen at critical concentrations: Part II – selected sensor test results. International Journal of Hydrogen Energy, 34(1): p. 562-571.

Buttner W., R. Burgess, M. Post, and C. Rivkin (2012), Summary and Findings from the NREL/DOE Hydrogen Sensor Workshop, in NREL/TP- 5600-55645

Cariteau B. And Tkatschenko I. (2013), Experimental study of the effects of vent geometry on the dispersion of a buoyant gas in a small enclosure, International Journal of Hydrogen Energy, 38(19): 8030-8038

Chernyavsky B., Hooker P., Hall J., Kuznetsov M. and Molkov V. (2014), Vent sizing correlation for mitigation of hydrogen-air deflagrations in low strength equipment and buildings, in preparation

Department of the Army (1969), Nuclear Handbook for Medical Service Personnel. Technical Manual TM8-215 (1969).

DNV Technica (2001), Human resistance against thermal effects, explosion effects, toxic effects and obscuration of vision. Technica DNV, 2001.

Finkel M.F. (2006), The neurological consequences of explosives, *Journal of the Neurological Sciences,* 249 (2006): 63-67.

Friedrich, A., Grune, J., Jordan, T., Kotchourko, A., Kotchourko, N., Kuznetsov, M., Sempert, K., Stern, G. (2007), Experimental study of hydrogen-air deflagrations in flat layer, Intl. Conf. on Hydrogen Safety, 11 – 13 September 2007, San Sebastian, Spain.

Hansen O., Middha P., Marangon A., Carcassi M., Ham K., Versloot N. (2007), Description of a Gaseous Hydrogen Refueling Station - Benchmark Base Case (BBC) for HyQRA IP 3.2. HyQRA BBC Station description (V1) (2007) 1-14.

Heitsch M., Baraldi D., Moretto P. (2010), Numerical analysis of accidental hydrogen release in a laboratory, Int. J. Hydrogen Energy, 35(9), pp. 4409-4419.

HSE (2006), Health and Safety Executive, Indicative human vulnerability to the hazardous agents present offshore for application in risk assessment of major accidents. SPC/Tech/OSD/30.

Hübert, T., et al. (2011), Hydrogen sensors – A review. Sensors and Actuators B: Chemical, 157(2), 329-352

HySafe (2007), Biannual report on hydrogen safety, HySafe; June 2007.

IEC 60079-29-1:2007 Explosive atmospheres – Part 29-1: Gas detectors- Performance requirements of detectors for flammable gases

IEC 60079-29-2:2007 Explosive atmospheres – Part 29-2: Gas detectors- Selection, installation, use and maintenance of detectors for flammable gases and oxygen

IEC 61779-6: Electrical apparatus for the detection and measurement of flammable gases – Part 6: Guide for the selection, installation, use and maintenance of apparatus for the detection and measurement of flammable gases. 2003

IEC 62282-3-100:2012 Fuel cell technologies - Part 3-100: Stationary fuel cell power systems – Safety Edition 1

ISO/PDTR 15916 (2008), Basic considerations for the safety of hydrogen systems, ISO TC 197 N 616 Second edition.

ISO 26142:2010 Hydrogen detection apparatus -- Stationary applications

Jarrett D.E. (1968), Derivation of British Explosive Safety Distances, *Annals of the New York Academy of Sciences*. 152 (1968) 18-35.

Jeffries R.M., Hunt S.J., Gould L. (1997), Derivation of fatality probability function for occupants buildings subject to blast loads (1997).

Jessel, W. (2002), Planning and Designing Gas Detection Systems. Sensors Mag., 19(1)

Korotcenkov, G. and B.K. Cho (2011), Instability of metal oxide-based conductometric gas sensors and approaches to stability improvement (short survey). Sensors and Actuators B: Chemical, 156(2), p. 527-538

Lamoureaux N., Djebaili-Chaumeix N., and Paillard C.-E. (2003), Flame velocity determination for H_2-air-He-CO_2 mixtures using the spherical bomb, *Exp. thermal and fluid sc*., 27 (2003), 385-393.

Lees F.P. (1996), Loss prevention in the process industries, 2nd Ed., Butterworth-Heinemann, Oxford, UK, 1996.

Linden PF (1999), The fluid mechanics of natural ventilation – Annu. Rev. Fluid Mech. – 1999 – 31, 201-238.

Lowesmith B.J., G. Hatkinson, C. Spataru, M. Stobbart (2007), - Gas build-up in a domestic property following release of methane/hydrogen mixtures. ICHS2 San Sebastian (2007)

Mercx W.P.M., Weerheijm J., Verhagen T.L.A. (1991), Some considerations on the damage criteria and safety distances for industrial explosions, 11th Symposium on New Directions in Process Safety - Hazards. 124 (1991) 255-275.

Molkov V. (1996), Venting gaseous deflagrations, D.Sc. thesis, 1996.

Molkov V, R Dobashi, M Suzuki, T Hirano (1999) Modeling of vented hydrogen-air deflagrations and correlations for vent sizing – Journal of Loss Prevention in the Process Industries, 12, 147-156

Molkov V. (2012), Fundamentals of hydrogen safety engineering, www.bookboon.com, 2012.

Molkov V. and Saffers J.-B. (2013), Hydrogen jet flames, I*ntl J. of Hydrogen Energy*, 38(19), 2013: 8141-8158.

Molkov V.V. and Bragin M. (2013), Hydrogen-air deflagrations: vent-sizing correlation for low-strength equipment and buildings, Intl. Conf. on Hydrogen Safety, Sept. 9-11, 2013, Brussels, Belgium.

Molkov V.V., Verbecke F. and Saffers J.-B. (2007), Uniform hydrogen-air deflagrations in vented enclosures and tunnels: predictive capabilities of engineering correlations and LES, 7th Intl. Symp. On Hazards Prevention and Mitigation of Industrial Explosions, July 7-11, 2007, St. Petersburg, Russia.

Molkov V.V., Shentsov, V., and Quintere, J. (2014), Passive ventilation of a sustained gaseous release in an enclosure with one vent, *Intl J. of Hydrogen Energy*, 39(15), 15 May 2014, 8158-8168.

NFPA (1998) National Fire Protection Association – NFPA 68 Guide for venting of deflagrations – Quincy, MA, USA – 1998.

NFPA 853 Installation of Stationary Fuel Cell Power Systems -2010 edition

NATO (1993), NATO, Field manual, health service support in a nuclear, biological, and chemical environment. fm 8-10-7 Headquarters, Department of the Army, Washington, D.C. (1993).

Palmisano(1), V., Weidner, E. Boon-Brett, L., Bonato, C., Harskamp, F. (2014), HyIndoor Final Report. WP5: SENSORS

Palmisano(2), V., Boon-Brett, L., Bonato, C., Harskamp, F., Buttner, W.J., Post, M.B., Burgess, R., Rivkin C. (2014), Evaluation of Selectivity of Commercial Hydrogen Sensors. accepted by Int. J. Hydrogen Energy

Palmisano(3), V., Weidner, E., Boon-Brett, L., Bonato, C., Harskamp, F., Buttner, W.J., Post, M.B., Burgess, R., Rivkin C. (2014), Selectivity and Resistance to Poisons of Commercial Hydrogen Sensors, in WHEC 2014: Gwangju

Pasman H.J. (2006), The challenge of risk control in a hydrogen based economy, Proceedings of the 1st European Summer School on Hydrogen Safety (2006).

César Porras-Amores, F.R.M., Ignacio Cañas (2014), Study of the Vertical Distribution of Air Temperature in Warehouses. Energies, 7: p. 1193-1206.

Raimundo A.M., Figueiredo A.R. (2009), Personal protective clothing and safety of firefighters near a high intensity fire front, *Fire Safety Journal*, 44(4) 2009: 514–521.

Rivkin, C., et al. (2011), A national set of hydrogen codes and standards for the United States, International Journal of Hydrogen Energy, 36(3), 2736-2741

Ross M. (1997), Lean combustion characteristics of hydrogen-nitrous oxide-ammonia mixtures in the air, M.Eng. Thesis, California Institute of Technology, Pasadena, California, USA, 1997.

Safety Planning Guidance for Hydrogen and Fuel Cell Projects, U.S.D.F.C.T. Program, Editor 2010

Saffers J.-B. (2010), Principles of hydrogen safety engineering, Ph.D. Thesis, University of Ulster, Belfast, UK, 2010.

Saffers J.-B. and Molkov V.V. (2010), Toward hydrogen safety engineering for reacting and non-reacting releases, 8th Intl. Symp. on Hazards, Prevention and Mitigation of Industrial Explosions, Sept. 5-10, 2010, Yokohama, Japan.

Saffers J.-B. and Molkov V.V. (2014), Hydrogen safety engineering framework and elementary design safety tools, *Intl. J. of Hydrogen Energy*, 39 (2014), pp. 6268-6285.

Scilly N.F., High W.G. (1986), The blast effects of explosions, Proceedings of the 5th International Symposium on Loss Prevention and Safety Promotion in the Process Industries (1986), 39-1-39-15.

Stamps, D. W., Slezak, S. E., and Tieszen, S. R. (2006), Observations of the cellular structure of fuel-air detonations, *Combustion and Flame,* 144:289-298.

Stephens M.M. (1970), Minimising Damage to Refineries from Nuclear Attack, Natural and Other Disasters. Office of Oil and Gas, Department of Interior.

Technical Standard L1 (2010), The Air Tightness Testing Measurement Association, Technical Standard L1. Measuring air permeability of building envelopes (dwellings), October 2010 issue (http://www.attma.org/)

Tien C.L., Lee K.Y., and Stretton A.J. (2002), “Radiation Heat Transfer,” in SFPE handbook of fire protection engineering, 3rd ed., Quincy, Mass. : Bethesda, Md: National Fire Protection Association ; Society of Fire Protection Engineers.

Verbecke F. (2009), Formation and combustion of non-uniform hydrogen-air mixtures, Ph.D. Thesis, University of Ulster, Belfast, UK, 2009.

Worster M.G, H.E. Huppert (1983), Time dependent profiles in a filling box, Journal of Fluid Mechanics 1983, 132:457-466.

Yakhot V. (1988), Propagation velocity of premixed turbulent flames, *Comb. Sc. and Tech*., 60 (1988), 191-214.

Glossary

Accident is an unforeseen and unplanned event or circumstance causing loss or injury.

Deflagration and **detonation** are propagation of a combustion zone at a velocity that is respectively less than and greater than the speed of sound in the unreacted mixture.

Flammability range is the range of concentrations between the lower and the upper flammability limits. *The lower flammability limit* (LFL) is the lowest concentration of a combustible substance in a gaseous oxidizer that will propagate a flame. *The upper flammability limit* (UFL) is the highest concentration of a combustible substance in a gaseous oxidizer that will propagate a flame.

Hazard is a chemical or physical condition that has the potential for causing damage to people, property and the environment.

Hydrogen safety engineering (HSE) is application of scientific and engineering principles to the protection of life, property and environment from adverse effects of incidents/accidents involving hydrogen.

Incident is something that occurs casually in connection with something else.

Laminar burning velocity is the rate of flame propagation relative to the velocity of the unburned gas that is ahead of it, under stated conditions of composition, temperature, and pressure of the unburned gas.

Normal Temperature and Pressure (NTP) conditions are: temperature 293.15 K and pressure 101.325 kPa.

Separation distance is the minimum separation between a hazard source and an object (human, equipment or environment) which will mitigate the effect of a likely foreseeable incident and prevent a minor incident escalating into a larger incident.

Specific gravity is the ratio of the density of a substance to the density of a reference substance, both at the same temperature and pressure.

Reynolds number is a dimensionless number that gives a measure of the ratio of inertial to viscous forces.

Risk is the combination of the probability of an event and its consequence.

Under-expanded jet is a jet with a pressure at the nozzle exit which is above atmospheric pressure.

Abbreviations

CFD	Computational Fluid Dynamics;
H2SE	Hydrogen Safety Engineering;
LFL	Lower Flammability Limit;
NTP	Normal Temperature and Pressure;
PPP	Pressure Peaking Phenomenon;
QDR	Qualitative Design Review;
UFL	Upper Flammability Limit.

4. Appendixes

4.1 Appendix 1: General safety rules, strategies and best practices

4.1.1 Hydrogen safety relevant harm criteria

- Oxygen depletion: hydrogen concentration between 9% and 28% by volume would impart evacuation, and would be life threatening at above 42% (HySafe, 2007);
- Direct contact with the flame:
  - British standard (BSI 2004) recommends 115ºC as the threshold for pain from an elevated air temperature for exposure exceeding 5 minutes.
  - DNV (2001) proposed the following classification of temperature effects on occupants:
    - below 70°C, no fatal issue in a closed space except uncomfortable situation;
    - between 70°C and 150°C, the impact is dominated by difficulties to breath;
    - above 150°C, skin burns occur in less than 5 minutes. This is considered a threshold temperature for escape;
    - 309°C third degree burns for a 20 s ("death" limit).
  - Time to incapacitation in minutes as a function of air temperature (^{o}C) can be estimated by the following equations recommended by DNV (2001) and BSI (1997) respectively:

$$t_{incap} = 5.33 \cdot 10^{8} \cdot T_{air}^{-3.66} \quad (1.1)$$

$$t_{incap} = 5 \cdot 10^{7} \cdot T_{air}^{-3.4} \quad (1.2)$$

  - For the acceptance threshold temperature of 115^{o}C Eqs. (1.1) and (1.2) provide incapacitation time of 5 minutes and 15 minutes of exposure respectively.
  - Bryan (1986) and DNV (2001) provide more details on physiological response of humans to air at elevated temperature (Table 1):

Table 1. Effect of air temperature on people (Bryan, 1986; DNV, 2001).

Temperature	Effect on people
127°C	difficult breathing
149°C	mouth breathing difficult, temperature limit for escape
160°C	rapid, unbearable pain with dry skin
182°C	irreversible injuries in 30 seconds
203°C	respiratory systems tolerance time less than four minutes with wet skin
309°C	third degree burns for a 20 seconds exposure, causes burns to larynx after a few minutes, escape improbable

  - Figure 5 illustrates time to incapacitation as a function of duration of exposure calculated using Eqs. (1.1) and (1.2). Note that for the lower temperatures (the dash lines) the use of these equations is not relevant.

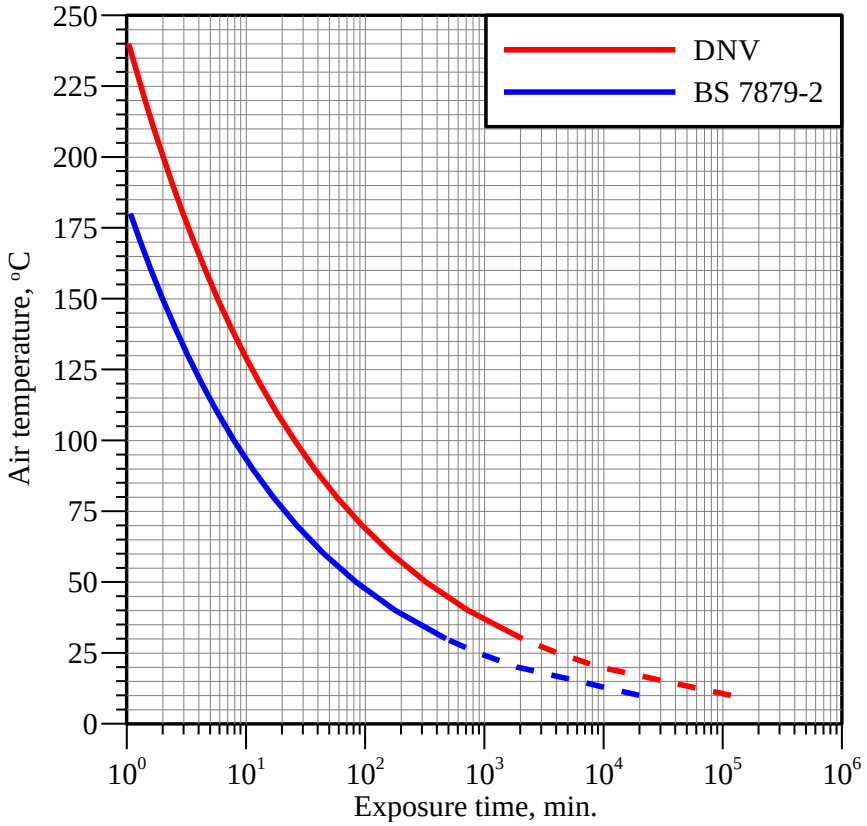

Figure 5. Time to incapacitation as a function of duration of exposure calculated using BSI (1997) – red curve, and DNV (2001) – blue line – approaches (Saffers, 2010).

- Radiant heat flux:
  - 1.5 kW/m^2 radiant flux is considered safe for the memebers of public (Saffers, 2010).
  - 2.5 kW/m^2 radiant flux is considered the tolerable value for building occupant. Pain and 1st degree burn will occur after 38 seconds exposure but do not prevent from evacuating (Saffers 2010). According to BSI (2004) this level of intensity can be withstood for more than 5 minutes.
  - 5 kW/m^2 radiant flux can be considered a threshold of tolerability for emergency responders with protective clothing (Saffers, 2010). Raimundo and Figueiredo (2009) set this value at 7 kW/m^2 and (Lees, 1996) at 4.7 kW/m^2. Long exposure should be avoided.
  - The maximum value for occupant can be set at 6 kW/m^2, as this intensity is lethal in about 38 seconds and pain is reach in just 12 seconds (Saffers, 2010).
  - Table 2 had been compiled by Saffers (2010) based on (Lees, 1996), (BSI, 2004), (Pasman, 2006) and (Raimundo and Figueiredo, 2009):

Table 2. Effect of radiant heat flux on people (Saffers, 2010).

Radiant heat flux (kW/m^2)	Effects on people
1.5	Intensity safe for stationery personnel and members of the public
2.5	Intensity tolerable over 5 min.; severe pain above this threshold
3	Intensity tolerable in infrequent emergency situations for 30 min.
5	Intensity tolerable for performing emergency operations
6	Intensity tolerable to escaping personnel
9.5	Second degree burn after 20 seconds
12.5 to 15	First degree burn after 10 seconds, 1% fatality in 1 minute
25	Significant injury in 10 seconds, 100% fatality in 1 minute
35 to 37.5	1% fatality in 10 seconds

- For buildings and structures, the light damages threshold can be set at 5 kW/m^2 as it is the intensity at which the windows break (Saffers, 2010).
- The moderate damages threshold could be set at 10 kW/m^2 (Saffers, 2010).
- Table 3 summarises the effects of intensity of radiant heat flux on structures and environment (Lees, 1996):

Table 3. Effects of radiant heat flux to structures and environment (Lees, 1996).

Radiant heat flux (kW/m^2)	Effects on structures and environment
5	Intensity for significant windows breakage
8-12	Intensity for domino effects
10	Heating of structures; increase of temperature and pressure in liquid/gas storages
10 – 12	Intensity for vegetation ignites
16	Intensity for failure of structures in prolonged exposure (except concrete)
20	Intensity concrete structures can withstand for several hours
30	Intensity for non-piloted ignition of wood occurs
38	Intensity for damages caused to process equipment and storage tanks
100	Steel weakening
200	Intensity for concrete structures to fail in several dozen of minutes

- Overpressure:
  - Overpressure can affect life safety through both direct (damage to persons from the overpressure itself) and indirect (damage produced by body displacement due to drag force, structural collapse and flying debris, such as glass shards from broken windows, etc.) effects.
  - Structures are more prone to be impacted by blast wave than people. Indirect damage to the occupants indoors (e.g. from the glass shards produced by broken windows) can require more stringent safety threshold than direct damage. NATO filed manual (NATO, 1993) states that the indirect blast injuries are so predominant that people exposed only to direct blast injuries make up a small part of the patient work load. Window panes are particularly easy to brake at very low pressures. Fragments can become missiles and impact people.
  - Saffers (2010) proposed 1 kPa as the tolerable value of overpressure for public indoors (Saffers, 2010). It corresponds to the breakage of 5% of windows as described in Table 6. 3 kPa is the threshold of injuries by glass fragment, while 10 kPa is the threshold of serious injuries by glass fragments. For comparison, when considering people outdoors, at 8 kPa, there are no serious injuries from direct impact of blast wave.
  - The maximum value of overpressure for occupants indoors can be taken as 10 kPa, above which there are serious injuries and some fatalities (Saffers 2010). For comparison, outdoors, at 8 kPa, there are no serious injuries from direct impact of blast wave and 21 kPa is the threshold of survivability. Lees (1996) cites Department of the Army (1969) in defined the range 15-20 kPa as the threshold for serious wounds outdoors.
  - The peak overpressure of 34 kPa is the threshold for eardrum rupture. This provokes deafness, tinnitus, and vertigo (Finkel, 2006), which would significantly impart evaculation.
  - Table 4 compiled by Saffers (2010) provides peak values of overpressure and associated level of injury to people indoors and outdoors based on data by (Hansen et al., 2007), (APPEA, 1998), (Jeffries et al., 1997) and (HSE, 2006).

Table 4. Classification of level of direct and indirect injury to people depending on overpressure (Saffers, 2010) from (Hansen et al., 2007), (APPEA, 1998), (Jeffries et al., 1997) and (HSE, 2006).

Overpressure (kPa)	Direct effects on people
8	No serious injury to people outdoors
10	Serious injuries to people indoors, few fatalities
21	Threshold of survivability 20% probability of fatality to people indoors 0% probability of fatality outdoors
30	Many fatalities indoors
34	Eardrum rupture
35	50% probability of fatality indoors 15% probability of fatality outdoors
54	Fatal head injury
62	Severe lung damage
70	100% probability of fatality indoors or in unprotected structures
82	Severe injury or death
	Indirect effects on people
3	Injuries by glass fragments to people indoors
6.9 – 13.8	Threshold of skin lacerations by missiles
10.3 – 20	People knocked down by pressure wave
13.8	Possible fatality by being projected against obstacles
27.6 – 34.5	50% probability of fatality from missile wounds
48.3 – 68.9	100% probability of fatality from missile wounds

- For the people outdoors, Barry (2003) provides the following estimate of peak values of overpressure and associated level of injury to people outdoor:

Table 5. Overpressure peak values and injury levels (Barry, 2003).

Overpressure	Injury level
8 kPa	no serious injury to people
6.9 – 13.8 kPa	threshold of skin lacerations by missiles
10.3-20 kPa	people are knocked down by pressure wave
13.8 kPA	possible fatality by being projected against obstacles
34 kPa	eardrum rupture
35 kPa	15% probability of fatality
54 kPa	fatal head injury
62 kPa	severe lung damage
83 kPa	severe injury or death

- Figure 6 shows the plots of the Probit functions for eardrum rupture and death by lung haemorrhage cited in Lees (1996) and for human fatality cited by HSE (2006).

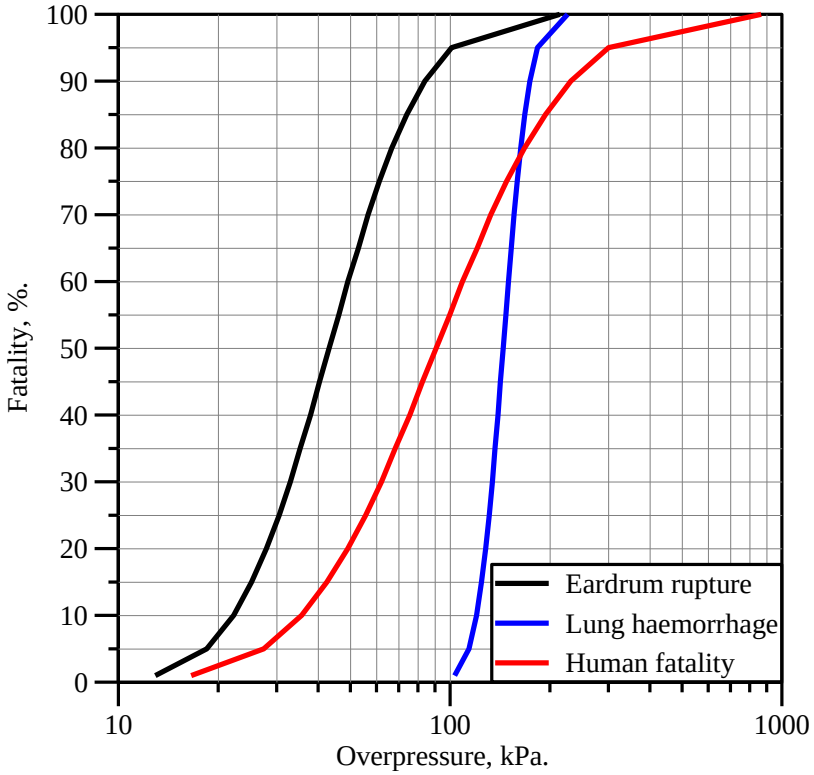

Figure 6. Probability of fatality, death by lung haemorrhage and eardrum rupture as a function of peak overpressure (Saffers, 2010).

- Table 6 compiled from Scilly and High (1986) and Lees (1996) summarizes the effect of overpressure on structures.

Table 6. Structural response to peak overpressure (Scilly and High, 1986), (Lees, 1996).

Elements	Overpressure (kPa)	Failure
Window pane	0.7 – 1	5 % broken
	1.4 – 3	50% broken
	3 – 6	90% broken
Building	1.4 – 3	Inhabitable after repair damage to ceilings, window and tiling
	3 – 6	Limited minor structural damage. Partitions and joinery was wrenched from fixings. Damage to house ceilings; 10% window glass broken.
	6 – 9	Doors and window frames broken in
	9	Steel frame of clad building slightly distorted
	14 – 28	Uninhabitable; partial of total collapse of roof, partial demolition of one or two external walls, severe damage to load-bearing partitions
		Concrete or cinder block walls, not reinforced, shattered
	30	Destruction of all buildings that were not designed to withstand explosions
	35 - 80	50% to 75% external brickwork destroyed or rendered unsafe
	80 - 26	Almost complete demolition
	50 - 100	Displacement of cylindrical storage, failure of pipes

- A pressure peak for domino effects may also be defined at a value of 20 kPa (Guide to the effects of accidents, 2004), and used as threshold when applying the Control of Major Accident Hazards (COMAH) Regulations (Saffers, 2010).
- The damages listed in the Table 6 can be classified and summarized as (Stephens, 1970):

Table 7. Classification of damages to structures depending on overpressure (Stephen, 1970).

Overpressure (kPa)	Damage level
<3.5	Light damage
>17	Moderate damage
>35	Severe damage
>83	Total destruction

- Blast wave effect depends on both peak overpressure and impulse. The following threshold values had been proposed (Saffers, 2010):
  - The sensitive area threshold would be set at 20 kPa.
  - The light damages threshold could be set at 3 kPa with an impulse greater than 100 Pa·s. At this overpressure, the infrastructure is inhabitable after repair damage to ceilings, window and tiling. For overpressure above 3 kPa but with an impulse lower then 100 Pa·s the threshold is shown in Figure 7.
  - The moderate damages threshold could be set at 15 kPa with an impulse greater than 300 Pa·s. For overpressure between 35 kPa and 15 kPa but with an impulse lower then 300 Pa·s refer to the Figure 7.
  - The collapse thresholds is set at 35 kPa with an impulse greater than 500 Pa·s. For overpressure higher than 35 kPa but with an impulse lower then 500 Pa·s it is recommended to refer to the Figure 7.

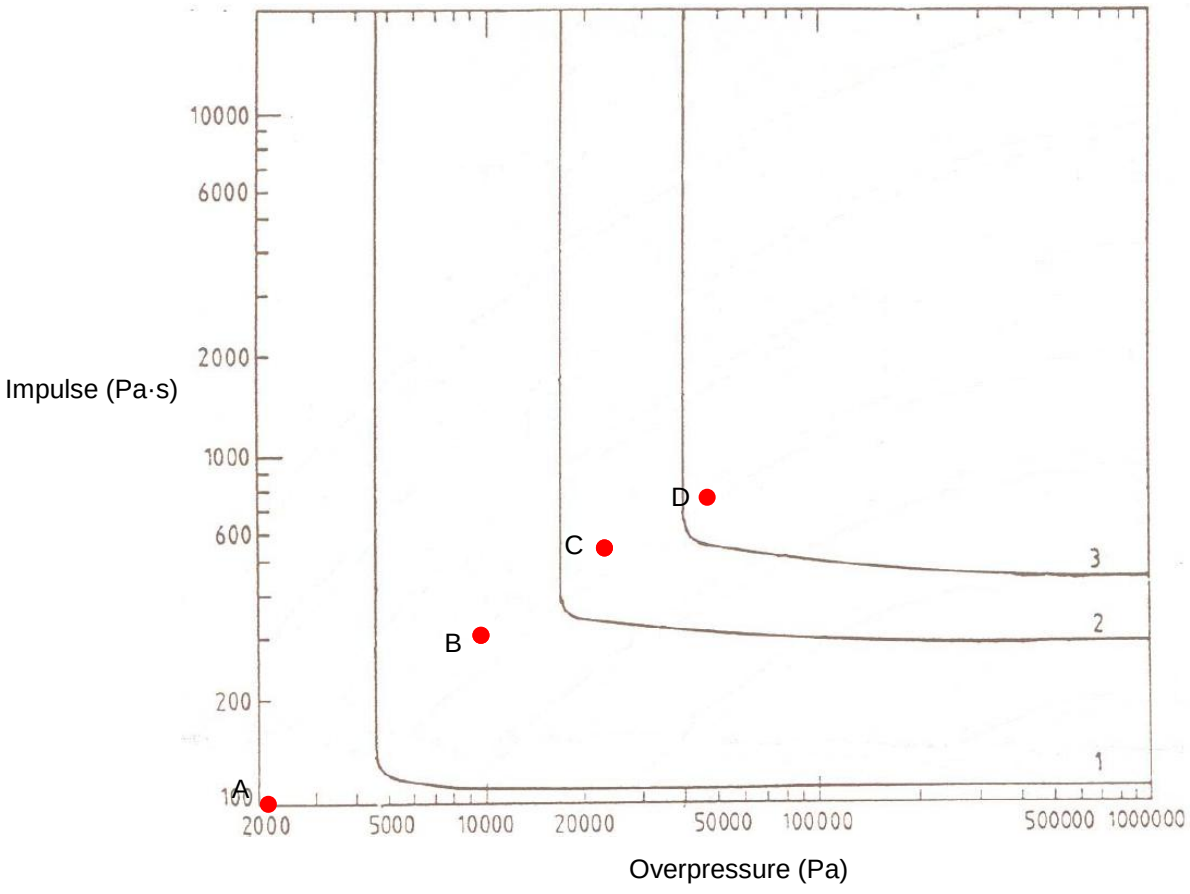

Figure 7. Overpressure-Impulse diagram of a high explosive charge on the ground, producing a gradual level of damage to houses: Level 1 light, level 2 structural damage and level 3 collapse (Mercx et al., 1991). Markers A,B, C and D corresponds to damage level thresholds described by Baker et al. (1983), and Jarrett (1968) (see

Table 8).

Table 8. Classification of damages to structures depending on overpressure and impulse (Baker et al., 1983, and Jarrett, 1968 via Saffers, 2010).

Peak overpressure (kPa)	Impulse (kPa·s)	Damage description	Representation in Figure 7
3.6	0.10	Border of minor structural damages	A
14.6	0.30	Threshold for moderate structural damages: some load bearing elements fail	B
34.5	0.52	Threshold for partial destructions: 50% to 75% of walls destroyed	C
70.1	0.77	Total destruction of buildings	D

- Cold burn from liquid hydrogen spill

Harm criteria discussed in this appendix can be briefly summarized in Table 9 and Table 10 (Saffers, 2010):

Table 9. Numerical values for the definition of acceptance criteria for life safety (Saffers, 2010).

Position	Hazard	Threshold	Occupant	Public	Fire-Fighter
Indoors and Outdoors	H_2 concentration (% by vol.)	Maximum	40		
		Tolerable	28	9	9
	Air temperature (^oC)	Maximum	149		
		Tolerable	115	70	149
	Direct radiant heat flux (kW/m^2)	Maximum	6		
		Tolerable	2.5	1.5	5
	Direct overpressure (kPa)	Maximum	34		
		Tolerable	21	8	8
Indoors	Indirect overpressure - missiles from windows (kPa)	Maximum	10		
		Tolerable	1	1	1
	Indirect overpressure - collapse (kPa)	Collapse	35	35	35
	Indirect radiant heat flux - collapse (kW/m^2)	Collapse	Material dependant		

Table 10. Numerical values for the definition of acceptance criteria for property loss (Saffers, 2010).

Hazard	Threshold	Values
Overpressure (kPa)	Collapse	35
	Moderate damages	15
	Light damages	6
	Sensitive area	20
Radiant Heat Flux ($kW \cdot m^{-2}$)	Collapse	Material dependant
	Moderate damages	10
	Light damages	3

	Sensitive area	10

4.1.2 Nomogram for concentration decay in momentum-dominated jet

Most of jet releases from hydrogen system are expected to be momentum dominated. Buoyancy-controlled jets decay faster compared to momentum–dominated (Molkov, 2012). Thus, calculation of decay in momentum-dominated jet can be accepted as a conservative estimate of decay in buoyant jet. The nomogram for calculation of concentration decay in unignited jet (Figure 8) is based on the similarity law widely validated against high pressure hydrogen releases from sources of different diameter (Molkov, 2012). The nomogram allows calculation of the necessary deterministic separation distance. It can be used to develop engineering solution to prevent generation of the layers with hydrogen concentration exceeding LFL under the ceiling, e.g. of a warehouse, based on the known storage pressure and leak diameter, e.g. tubing diameter.

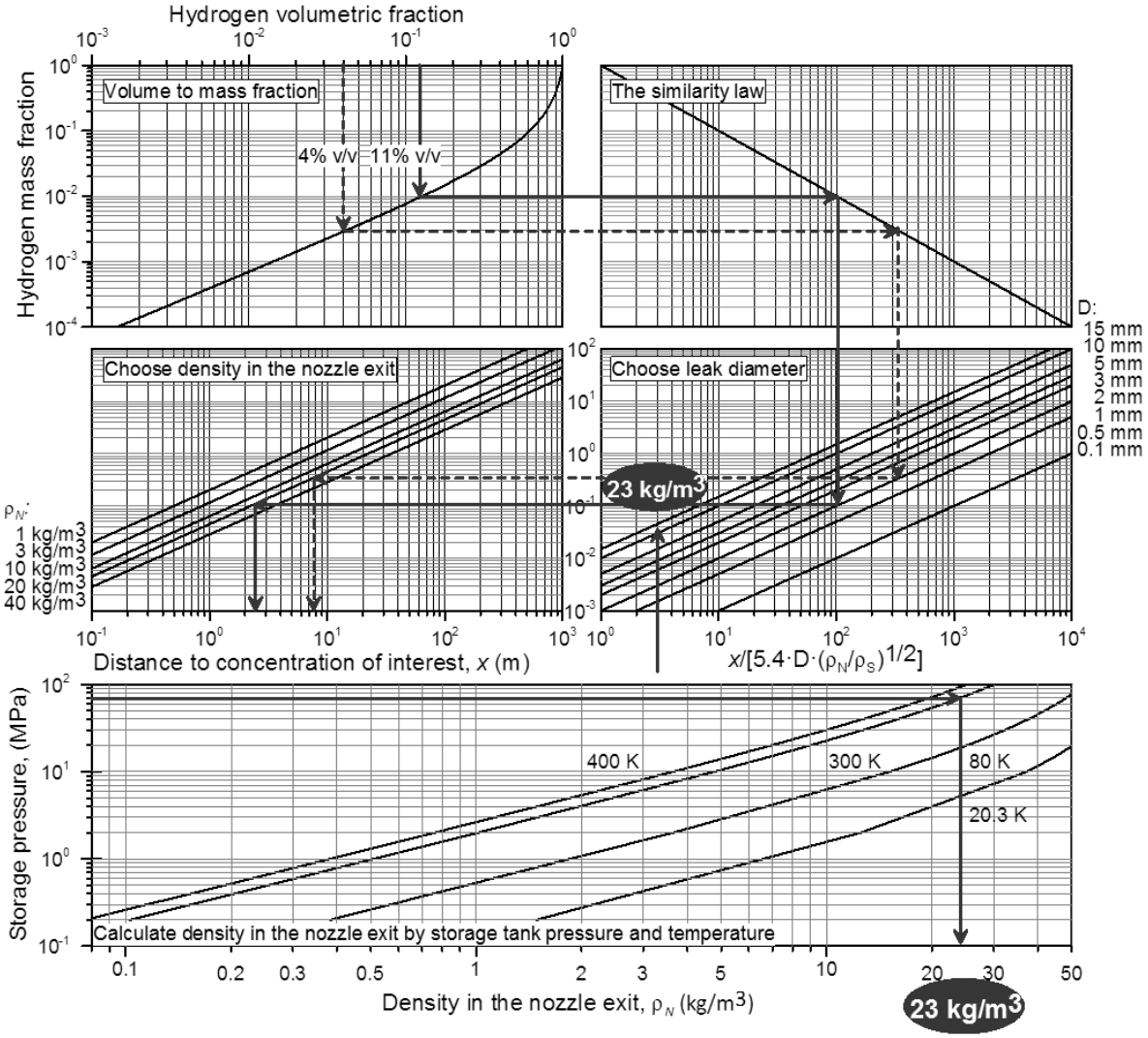

Figure 8. Nomogram of concentration decay in unignited jet (Molkov, 2012).

The procedure for nomogram utilization can be demonstrated on the example of calculation of distance to 4% hydrogen concentration by volume (dashed line corresponds to the lower flammability limit of hydrogen in air) and 11% by volume (solid line, corresponds to the average location of a jet flame tip) along the axis of

a release from a storage tank at pressure 70 MPa and temperature of hydrogen in a tank 300 K through a 1 mm diameter nozzle:
The calculation requires 6 steps as in the following ***example***:

- Firstly, the line from the axis “Hydrogen volumetric fraction” is drawn downwards from the chosen concentration of interest (4% and 11% by volume in our example) until the intersection with the line of the top left graph “Volumetric to mass fraction”.
- Secondly, the horizontal line from this intersection point is drawn to the intersection with the similarity law line at the right top graph “The similarity law”.
- Thirdly, the vertical line is drawn downwards until intersection with line “1 mm” at the graph “Choose leak diameter”. There are eight lines on “Choose leak diameter” graph which correspond to the leak diameters of (from top to bottom) 15 mm, 10 mm, 5 mm, 3 mm, 2 mm, 1 mm, 0.5 mm, and 0.1 mm. The legend is shown at the right side of the graph.
- The fourth stage is to calculate the density using the additional graph “Calculate density in the nozzle exit by storage tank pressure and temperature” at the bottom of the nomogram using given pressure (70 MPa) on the ordinate axis and a line corresponding to the chosen temperature of stored hydrogen (300 K). This is shown by two thick grey lines on the “Calculate density in the nozzle exit by storage tank pressure and temperature” graph. Calculated graphically density at the nozzle exit for 70 MPa and 300 K is about 23 kg/m^3.
- The calculated value of density of 23 kg/m^3 is applied at the fifth stage of calculations to draw the horizontal line from the intersection with an imaginary line corresponding to 23 kg/m^3 at the “Choose density in the nozzle exit” graph (between two down on the graph lines 20 kg/m^3 and 50 kg/m^3). There are fine lines at the graph corresponding to densities 1, 3, 10, 20 and 50 kg/m^3 from top to bottom respectively. The legend is shown at the left side of the graph.
- The final stage is to draw the vertical line downwards from the intersection with the line 23 kg/m^3 to the intersection with abscissa axis of the “Choose density in the nozzle exit” graph. Thus, the calculated graphically distance from the nozzle exit to hydrogen concentration of 4% by volume is about 7.7 m, and to concentration of 11% by volume is about 2.7 m. The calculation by the equation for similarity law (Molkov, 2012) with the accurate value of the density at the nozzle calculated by the under-expanded jet theory (23.95 kg/m^3) and air density of 1.205 kg/m^3 (NTP) is 8.36 m for 4% and 2.83 m for 11%. The error of simple and fact graphical calculations of distances is at the acceptable level of below 10%.

4.2 Appendix 2: Ventilation of unignited releases

4.2.1 Pressure Peaking Phenomena

4.2.1.1 Nomogram to determine a leak rate leading to 100% of hydrogen in the enclosure

Pressure peaking phenomena is only observed in the case when the hydrogen release rate is sufficiently high to completely displace air from the enclosure with time of sustained leak. Therefore, before estimating overpressure produced by pressure peaking phenomenon (and applying the engineering tool described below) it is necessary to confirm that the release rate is sufficient to fill enclosure with 100% of hydrogen if a leak is sustained. Nomogram in Figure 9 can be used to verify if this is indeed the case. The nomogram is derived using Eq. (2.3) in Appendix 4.2.2.1 (Molkov et al., 2014) using discharge coefficient, C_D, of 0.85. The nomogram allows one to calculate the maximum vent dimensions which for a given steady release will eventually result in 100% hydrogen concentration in the enclosure. In order to find this maximum vent dimensions, select hydrogen release rate on the vertical axis and draw horizontal line until intersection with one of the lines corresponding to appropriate vent width. Draw vertical line from intersection point to horizontal axis to find required vent height. Alternatively, the nomogram in Figure 9 can be used to find minimal release rate for a known vent size when calculation of PPP is needed, in which case the above steps are reversed.

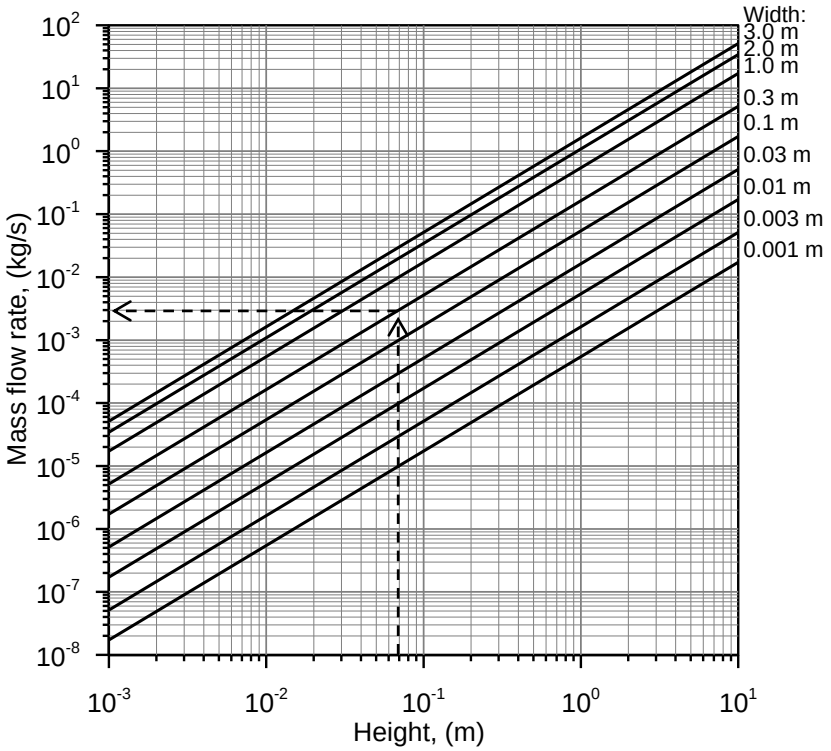

Figure 9. The nomogram for graphical calculation of hydrogen leak mass flow rate in an enclosure with one vent, which leads to 100% of hydrogen concentration, by the vent height and width (Molkov et al., 2014).

If release rate found through the nomogram is lower than actual release rate, or the actual vent dimensions are smaller than found using nomogram in Figure 9, 100% hydrogen concentration will be achieved and pressure peaking phenomena can occur.

Example

Consider the enclosure with 0.3 x 0.07 (W x H) m vent. What minimal hydrogen flow rate would be necessary to achieve 100% hydrogen concentration in the enclosure? To determine this rate, start from the horizontal axis and draw vertical line from the 0.07 m height mark upward, until intersection with diagonal width line corresponding to 0.3 m value. From the intersection point draw horizontal line left – the minimal hydrogen flow rate, needed to achieve 100% hydrogen concentration, can be read from the vertical axis (approximately 0.003 kg/s).

4.2.1.2 Nomograms for determination of overpressure due to pressure peaking phenomena

Figure 10 shows a nomogram for pressure peaking phenomenon calculation which allows calculation of the maximum overpressure peak produced by high rate hydrogen release from the known mass flow rate and leak diameter.

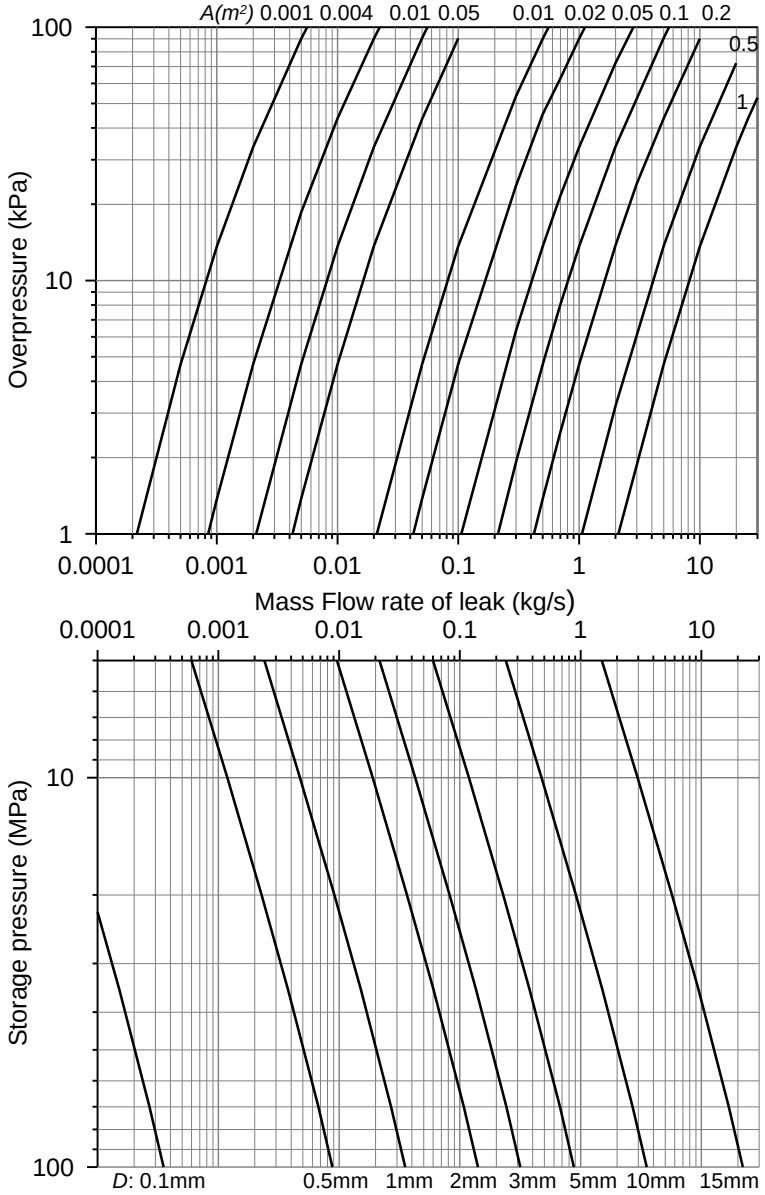

Figure 10. Pressure peaking nomogram for various release rates.

To use the nomogram in Figure 10, follow the following procedure:

- Start with the vertical axis on the lower panel of the graph and select storage pressure, read across horizontally to the leak diameter.
- Read vertically upwards to calculate the mass flow rate of the leak. Continue vertically upward from the mass flow rate to the point of intersection with the line for the appropriate vent area in the upper panel.
- Read horizontally to the left until intersection with vertical axis. The point of intersection provides the overpressure in the enclosure.
- Alternatively, the nomogram can be used to determine vent area required to keep overpressure below specified limit. In this case, follow the first two steps and then draw a horizontal line from the desired overpressure value found on the vertical axis of upper panel. Closest to the intersection curve in the upper panel will correspond to the required vent area (if the intersection falls between two curves, use rightmost in order to get conservative value).

4.2.1.3 *Nomograms for determination of 'safe' tubing diameter and blowdown duration with account for pressure peaking phenomenon*

Nomograms shown in Figure 11 and Figure 12 allow calculation of "safe" tubing diameter, i.e. such diameter which would not result in an overpressure exceeding 20 kPa in an enclosure in case of a leak, and the blowdown time with this releasing diameter. (Brennan and Molkov, 2013).

In order to use these nomograms it is necessary first to calculate the appropriate values of Air Change per Hour (ACH) in an enclosure of interest. The ACH is defined as the ratio of the volumetric air flow rate per hour, Q_{hr} (m^3/hr), and the enclosure volume, V (m^3), as

$$ACH = Q_{hr} / V \tag{2.1}$$

Bernoulli's equation can be used to express volumetric flow rate per second Q_s as a function of a vent area A (m^2) density of air ρ (kg/m^3) and pressure differential between the volume of the enclosure and the atmosphere ΔP (Pa), i.e.

$$Q_s = CA\sqrt{2\Delta P / \rho} \tag{2.2}$$

where C_D is the discharge coefficient. For derivation of nomograms in Figure 11 and Figure 12, a value of C_D = 0.6 had been used (Emmons 1995). Nomograms in Figure 11 and Figure 12 use the value of 50 Pa for ΔP. This value had been selected as it is utilized in 'n50' standard measurement used to determine air leakage rate in the residential buildings (Technical Standard L1, 2010). It should be noted, however, that this value is relatively high and lower values had been suggested by some researchers, e.g. 4 Pa recommended by Baker et al. (1987).

Figure 11 and Figure 12 allow one to estimate "safe" releasing diameter and blowdown duration for various initial hydrogen inventories in the storage tank, initial storage pressures, and ACH values. Nomograms in Figure 11 and Figure 12 are derived for the release from a tank containing 1, 5 and 13 kg of hydrogen, respectively, at 35 and 70 MPa. In order to determine "safe" releasing diameter, select the volume of the enclosure on the vertical axis of the lower panel and draw horizontal line until intersection with a curve corresponding to appropriate ACH and tank pressure. Projecting the vertical line from the intersection point to the horizontal axis will provide 'safe' tubing diameter in millimetres.

Continuing vertical line up until the intersection with appropriate curve in the upper panel provides estimate of the time required for overpressure in the tank to drop from initial to 0.1 MPa, i.e. blowdown duration. Duration in seconds can be read on the vertical axis of the upper panel.

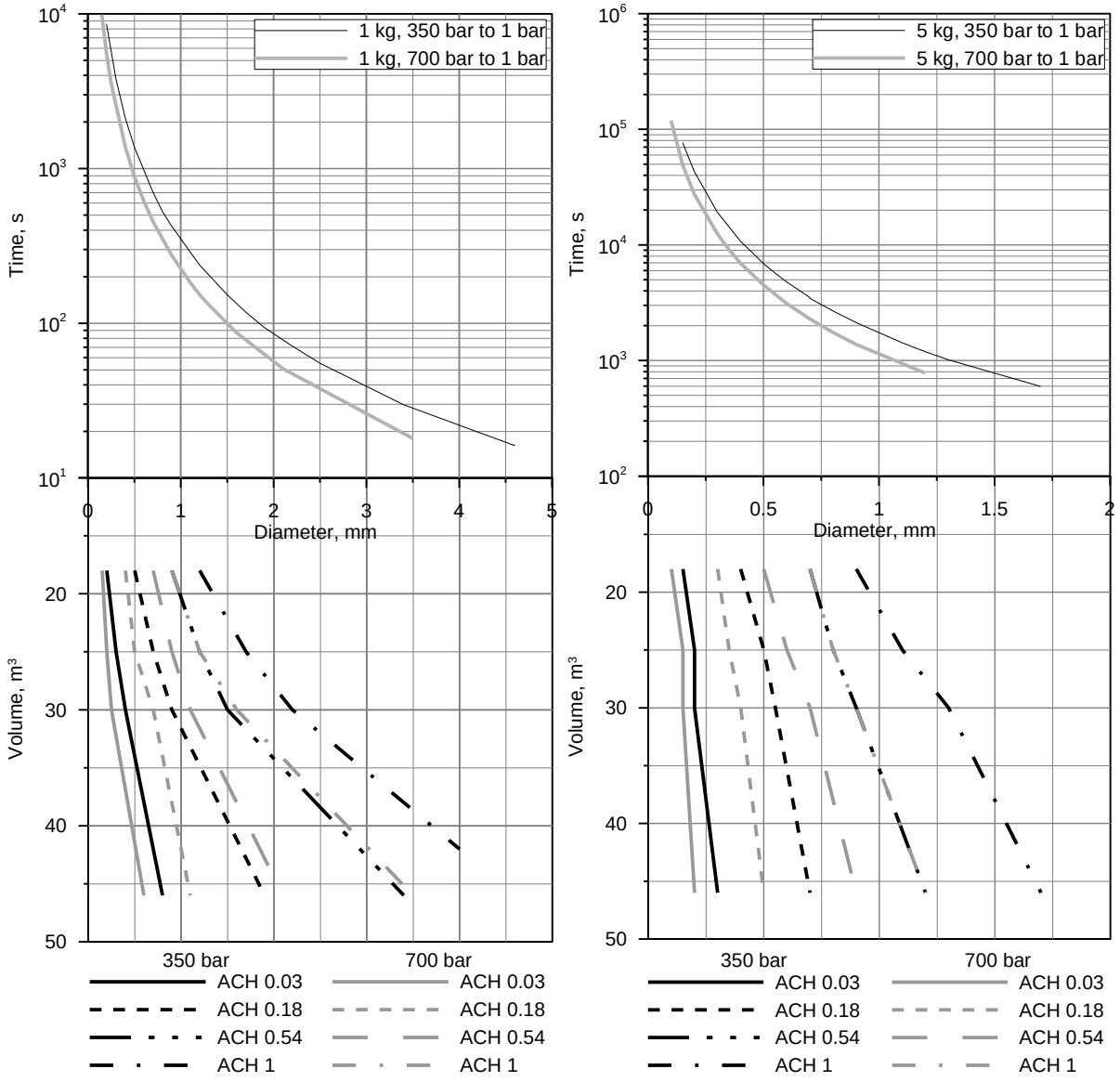

Figure 11. Nomogram for 'safe' diameter and blowdown duration from a tank containing 1 kg and 5 kg of hydrogen at 350 and 700 bars (Brennan and Molkov, 2013).

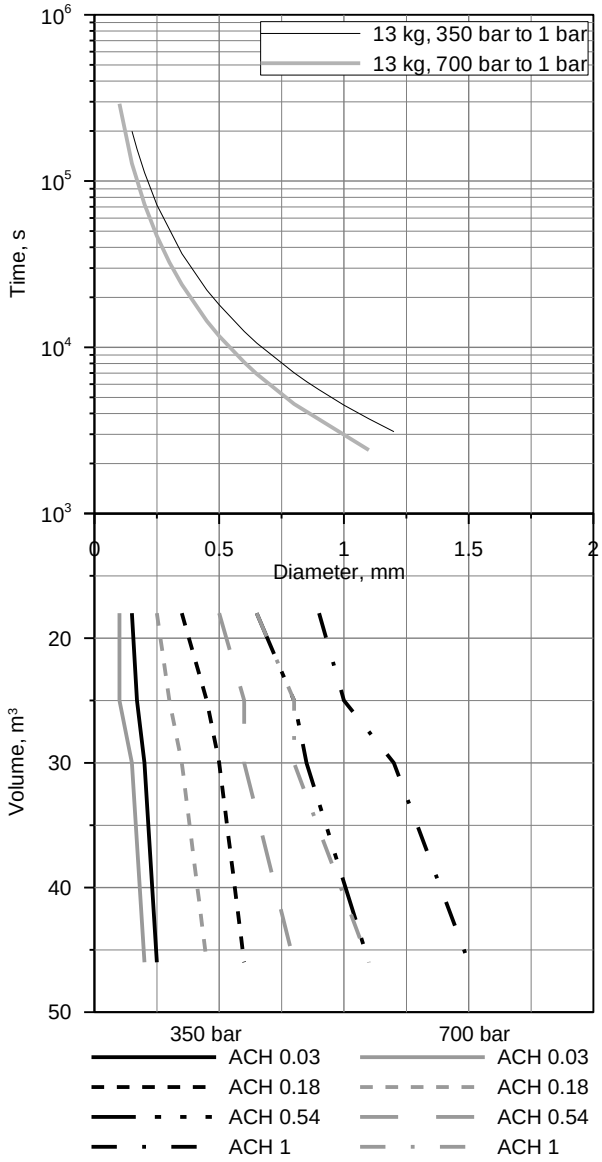

Figure 12. Nomogram for 'safe' diameter and blowdown duration from a tank containing 13 kg of hydrogen at 350 and 700 bars (Brennan and Molkov, 2013).

Example

Let us consider blowdown from the tank containing 5 kg of hydrogen under 700 bars into the 30 m^3 enclosure with ACH equal unity. First, one draws horizontal line from 30 m^3 mark on the vertical axis in the lower panel of Figure 11 until intersection with the curve corresponding to ACH 1 for 700 bar tank. Drawing vertical line from intersection up, one finds "safe" tubing diameter (approximately 0.875 mm). Continue line further up, until it intersects a curve corresponding to blowdown of 700 bar tank. Draw horizontal line from the intersection point and find the time required for blowdown from 700 to 1 bar – approximately $1.5 \cdot 10^3$ seconds.

4.2.1.4 Pressure peaking phenomenon for reacting mixture

During combustion of hydrogen in air water vapour produced as a product. Hydrogen has a higher adiabatic premixed flame temperature for a stoichiometric mixture in air of 2403K. One gram of burned hydrogen produces 9 g of water vapour. Density of water vapour based on the ideal gas equation of state $\rho = MP/RT$, where *M* is the molar mass (g/mole), *P* is the pressure (Pa), *T* is the temperature (K), and R is universal gas constant (8314.4 J/K/kmol) at T=2403 K is equal to 0.091 kg/m^3 and density of the released hydrogen at 273 K is 0.089 kg/m^3 which is close to the density of hot water vapour.

This means that the same approach as for the unignited pressure peaking phenomenon calculation described in Appendix 4.2.1.2 can be applied for jet fires just by increasing the mass flow rate of "unignited" hydrogen multiplying it by the factor of 10. This "rule of thumb" is useful engineering tool for assessment of pressure peaking phenomenon (PPP) for jet fire by using available model for PPP for unignited release.

4.2.2 Uniform mixtures – One-opening ventilation mode

4.2.2.1 Equations and nomogram for steady state concentration in enclosure with one vent

Maximum hydrogen concentration level in the enclosure with one vent in the assumption of sustained leak can be evaluated using the following equation (Molkov et al., 2014)

$$X = f(X)\cdot\left[\frac{Q_0}{C_D A(g'H)^{1/2}}\right]^{2/3}, \qquad (2.3)$$

where X is the hydrogen volume fraction, Q_0 is the release rate (m^3/s), C_D is discharge coefficient, A is vent area (m^2), H is vent height (m), g' is reduced gravity $g' = g(\rho_{air} - \rho_{h2})/\rho_{air}$ (m/s^2), ρ_{air} and ρ_{h2} are density of the air and hydrogen, respectively, (kg/m^3) and function $f(X)$ is equal

$$f(X) = \left(\frac{9}{8}\right)^{1/3}\left\{\left[1 - X\left(1 - \frac{\rho_{h2}}{\rho_{air}}\right)\right]^{1/3} + (1-X)^{2/3}\right\}. \qquad (2.4)$$

Eq. (2.3) is derived in assumption that:

- The release flow rate remains constant;
- Gas mixture is uniform across the enclosure, i.e. hydrogen concentration is not a function of location inside the enclosure.

Comparison with experiments had shown, however, that Eq. (2.3) can be used to predict the maximum hydrogen concentration in the case of hydrogen forming layers (Molkov et al., 2014), i.e. it can be considered conservative.

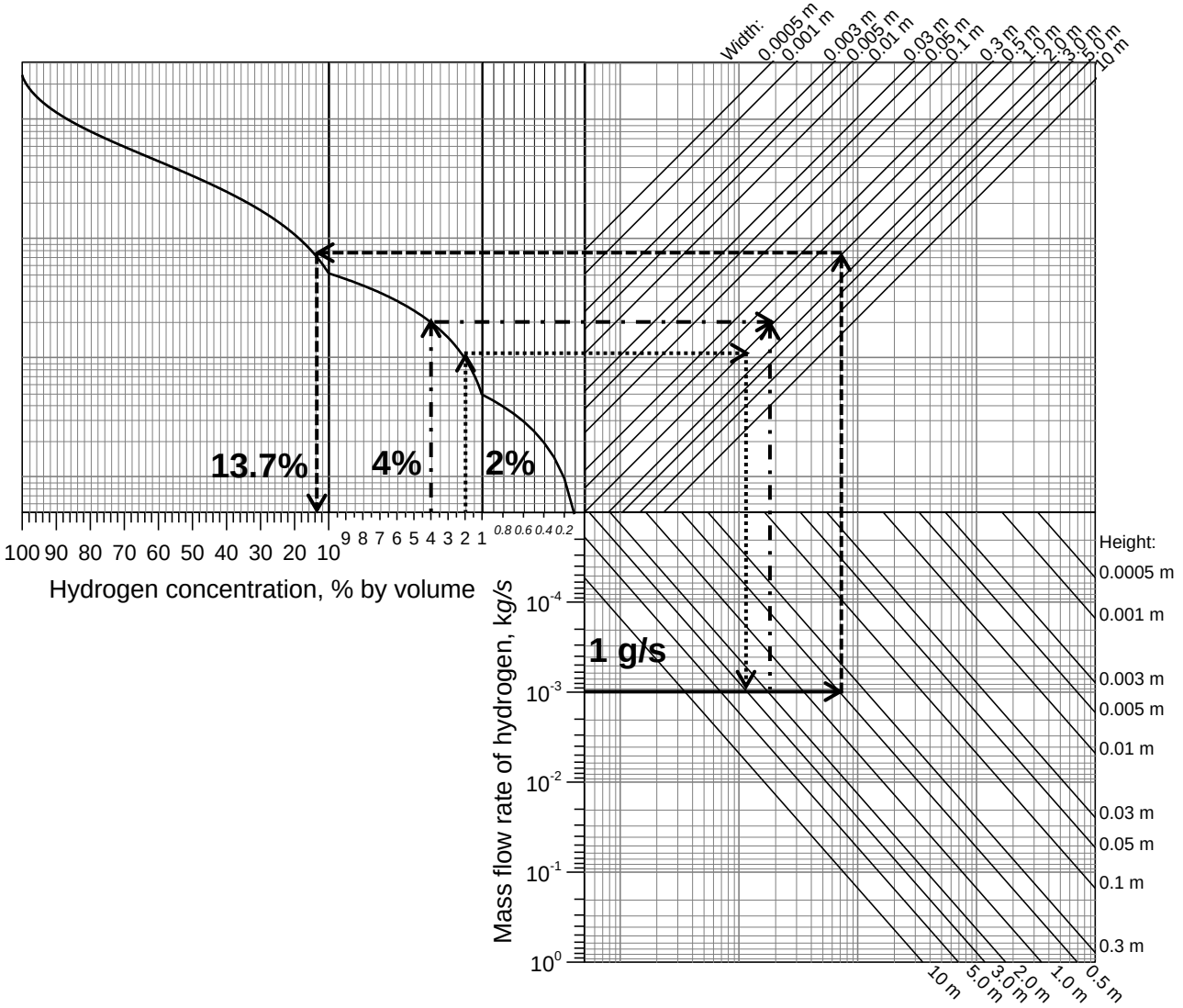

Figure 13. Nomogram for calculation of maximal value of steady state concentration in the enclosure with one vent.

Figure 13 shows an engineering nomogram that is a graphical representation of Eq. (2.3) with determined value of discharge coefficient C_D=0.6. The nomogram can be used to calculate hydrogen maximum concentration at steady state condition by known height and width of a vent and release rate. The nomogram is valid for both uniform and non-uniform mixtures in an enclosure with one vent. The procedure for hydrogen concentration calculation is as follows (follow dashed line in B2.1):

- Select the mass flow rate of hydrogen leak at the vertical axis of the lower panel of the nomogram and project it horizontally until intersection with one of the diagonal lines corresponding to different vent heights. There are 15 such lines in the nomogram in Figure 13, covering practically all possible vent heights between 0.5 mm and 10 m.
- From the point of intersection, draw a vertical line up until intersection with one of the diagonal lines in the top right panel of the nomogram, which corresponds to various vent widths. There are 15 such lines in the nomogram in Figure 13, covering vent widths between 0.5 mm and 10 m.
- From the point of intersection, draw a horizontal line left until intersection with the function curve in the top left panel of the nomogram.
- Draw a vertical line from the point of intersection to the horizontal axis of the top left panel. The value on the horizontal axis would correspond to the hydrogen concentration % by volume.

The nomogram in Figure 13 can also be used for the opposite calculation, i.e. for calculation of the vent size required to ensure that for the given hydrogen release rate the concentration will not exceed specified values

(see dash-dotted and dotted arrows in Figure 13). In this case the process of calculation is performed in the reverse order, starting with desirable concentration value (see example with 2% mixture in Figure 13).

Example

Let us consider the enclosure with a single 1 x 0.5 (W x H) m vent, with a steady release of the hydrogen at a rate of 1 g/s. Let us further assume that the hydrogen-air mixture is well mixed and the gas concentration is uniform across the entire enclosure. Following the procedure described above we can use nomogram in Figure 13 to find what would be the steady state concentration of the hydrogen in the enclosure as follows:

1. Select flow rate (1 g/s) on the vertical axis in the lower right panel of the nomogram. Draw horizontal line until intersection with the diagonal line corresponding to our vent height – 0.5 m (solid arrow in Figure 13);
2. From the intersection, draw vertical line up until intersection with diagonal line in the upper right panel of the nomogram, corresponding to vent width – 1 m (dashed arrow);
3. Draw horizontal line from the point of intersection to the left until it meets the function curve in the upper left panel (dashed arrow);
4. Draw vertical line down from the intersection (dashed arrow) and read the steady state hydrogen volume percentage value on the horizontal axis of upper left panel – 13.7%.

Conversely, if one wanted to find vent dimensions required to keep hydrogen volume percentage below a certain value – e.g. 2% (dotted line arrows) or 4% (dash-dotted line arrows) – one would start with the desired volume percentage value at the horizontal axis of the upper left panel and draw vertical line until intersection with the function curve in this panel. From there one can draw horizontal line to the right toward upper right panel, passing across vent width curves. Next, one should select the release mass flow rate (e.g. 1 g/s) in the lower left panel of the nomogram, drawing horizontal line to right across lower right panel, passing through vent height curves. It is now possible to determine the dimensions of the vent required for maximum hydrogen concentration by volume to not exceed 2% or 4% value for a specified hydrogen release.

Let us consider two cases with the same release rate of 1 g/s. In the first case (maximum allowable concentration of hydrogen 4% by volume, dash-dotted arrows), let us assume that vent width is fixed at 1 m. Required vent height can be determined by starting at the point of intersection between horizontal line drawn across upper right panel and diagonal line corresponding to 1 m vent width, and drawing vertical line down toward lower right panel until intersection with horizontal line corresponding to selected flow rate. If the intersection falls between two diagonal vent height lines, the desired height lies between two values corresponding to these lines. For our example, required vent height would be approximately 1.8 m (intersection point lies close to 2 m height curve). Therefore the dimensions of the vent which would ensure 4% hydrogen volume percentage for 1 g/s release are 1 x 1.8 (W x H) m.

In the second case (maximum allowable concentration of hydrogen 2% by volume, dotted arrows), let us assume that both vent height and width are free parameters. In order to determine vent dimensions, let us draw a vertical line connecting horizontal lines originating from specified release rate (in the lower right panel) and from the concentration level/function curve intersection (in the upper right panel). The values indicated on diagonal curves nearest to the intersections between these horizontal lines and connecting vertical line will correspond to vent height (in the upper right panel) and width (in the lower right panel) values. If the intersection falls between two diagonal curves, the corresponding vent dimension will have a value lying between the values marked on these curves. By moving this line left or right, one can obtain different sets of (height, width) values, which will provide the same hydrogen concentration by volume for the given release rate. For an example shown in Figure 13, 2% hydrogen concentration requires the vent height of 3 m and the width of approximately 1.3 m.

4.2.2.2 *Equations for steady state concentration in enclosure with one vent from 1999 Linden approach through Cariteau and Tkaschenko (2013) formulation*

On the basis of the Linden work, as shown on Figure 14, a well-mixed regime is observed in an enclosure in case of buoyant gas release. Linden (1999) proposes a methodology to calculate the concentration at steady-state and the concentration evolution with time during the filling (during the release) and the drainage phase (after release end).

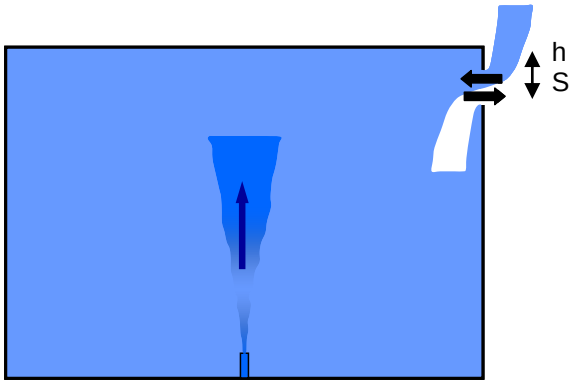

Figure 14. Schematics of the well-mixed regime obtained in case of ventilation by a single opening.

During the filling phase, the expression of the flow crossing the vent opening is given by:

$$Q = C_D S\left(g_0^{'}.h\right)^{1/2}, \tag{2.5}$$

with the reduced gravity (m.s^{-2}):

$$g_0^{'} = g.\left(\frac{\rho_a - \rho_0}{\rho_a}\right), \tag{2.6}$$

where C_D – vent discharge coefficient, constant value, h – vent dimension ,m, S – vent area, m^2, ρ_a – air density, kg.m^{-3}, ρ_0 – releasing gas (hydrogen) density, kg.m^{-3}.

It should be noticed that the gas molar fraction is:

$$X_f = \left(\frac{g^{'}}{g_0^{'}}\right), \tag{2.7}$$

where g' – reduced density of the gas in the enclosure (hydrogen diluted with air), m.s^{-2}.

Then, if the buoyancy conservation is applied ($g_0^{'}Q_0 = g^{'}Q$), the fraction of a buoyant gas leading to the steady state in a ventilated room with a single vent is given as follows:

$$X_f = \left(\frac{Q_0}{C_D S\left(g_0^{'}.h\right)^{1/2}}\right)^{2/3}, \tag{2.8}$$

where Q_0 – leaking gas flow rate, m^3.s^{-1}, a C_D of 0.25 is recommended for the use of the Eq. (2.8) to determine hydrogen concentration at steady state.

4.2.2.3 *Methodology to determine the appropriate flow rate of a mechanical/forced ventilation for one-opening enclosure*

Forced ventilation should be applied in cases when passive ventilation is impractical or insufficient.

Considering one-opening ventilation mode with uniform mixture, the Molkov et al. (2014) developments presented in Appendix 4.2.2.1 can also be used to evaluate the appropriate flow rate of mechanical/forced ventilation.

Waiting further advancement on this topic, a methodology is presented hereafter.

1. Mechanical/forced ventilation by extraction

For a case of uniform hydrogen concentration in the enclosure, required flow rate can be calculated as

$$Q_{FS} = \frac{Q_{H_2}}{X}$$ for the forced extraction of hydrogen-air mixture (2.9)

where *X* is the targeted maximal hydrogen volume fraction, Q_{H_2} is the hydrogen release flow rate and Q_{FS} is the required extraction flow rate [m^3/s].

In this case vent opened to atmosphere works for inflow only).

2. Mechanical/forced ventilation by blow-in

For a case of uniform hydrogen concentration in the enclosure, required flow rate can be calculated as

$$Q_{FB} = \frac{Q_{H_2}}{X}(1-X)$$ for the forced blow-in of the fresh air to dilute hydrogen-air mixture (2.10)

where *X* is the targeted maximal hydrogen volume fraction, Q_{H_2} is the hydrogen release flow rate and Q_{FB} is the blow-in flow rate [m^3/s].

In this case vent opened to atmosphere works for outflow only.

4.2.3 Layered mixtures – Two-openings ventilation mode

On the basis of the Linden work (Linden, 1999)), as shown on Figure below, a buoyant gas release in an enclosure with two ventilation openings leads to a displacement ventilation regime with the formation of an upper homogeneous concentration. Linden proposes a methodology to calculate the maximal concentration at steady-state.

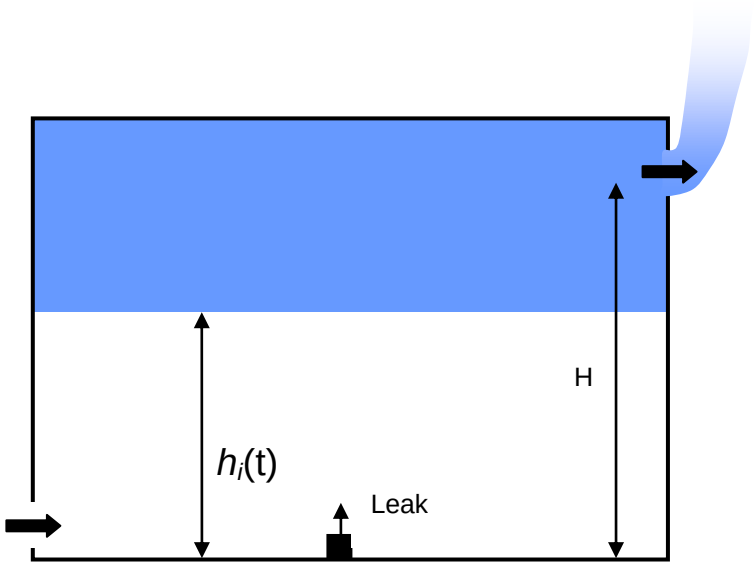

Figure 15. Schematics of the displacement regime obtained in case of natural ventilation by two openings.

Using the S_t and S_b, respectively the opening surfaces of the top and bottom openings, the effective opening area is:

$$S' = \frac{\sqrt{C_t} S_t S_b}{\left(\frac{1}{2} \left(\frac{C_t}{C_b} S_t^2 + S_b^2 \right) \right)^{1/2}}, \tag{2.10}$$

where C_t – top vent discharge coefficient, constant value, C_b – bottom vent discharge coefficient, constant value, constant value, S_t – top vent area, m^2, S_b – bottom vent area, m^2.

At steady state, the interface height, h_i, is given by:

$$\frac{S'}{H^2} = C^{3/2} \left(\frac{\xi^5}{1-\xi} \right)^{1/2}, \tag{2.12}$$

and:

$$\xi = \frac{h_i}{H}, \tag{2.13}$$

where H – height of the upper vent, m.
The height of the interface only depends on the geometrical configuration of the vents (size and height).

At steady state, the molar fraction in the upper layer is expressed by:

$$X_f = \frac{1}{C}\left(\frac{Q_0^2 h_i^{-5}}{g_0'}\right)^{1/3}, \quad (2.14)$$

where g_0' – reduced gravity, m.s^{-2}, C – constant value of 0.115 depending on the air entrainment coefficient α (0.10 is used herein for α in Linden approach formulation):

$$C = \frac{6}{5}\alpha\left(\frac{9}{10}\alpha\right)^{\frac{1}{3}}.\pi^{\frac{2}{3}} \quad (2.15)$$

It is important to notice that in this model the release is considered on the floor.

4.3 Appendix 3: Mitigation of hydrogen indoor deflagrations.

4.3.1 Simple thermodynamic model for inventory limitation

A simple thermodynamic model may be developed to predict maximum mass of hydrogen, which may be allowed to be released in an enclosure without causing destructive overpressure in case of its combustion. The model presumes that enclosure is partially filled with air, volume fraction of air is x_a, and partially – with unburnt hydrogen-air mixture, volume fraction x_u, initial pressure p_0. If this hydrogen-air mixture is burnt in a sealed enclosure, the solution for resulting absolute pressure p_2 may be found from equation from the following equation:

$$p_2 = x_u p_{b1}\left(\frac{p_2}{p_{b1}}\right)^{\frac{\gamma_b-1}{\gamma_b}} + x_a p_0\left(\frac{p_2}{p_0}\right)^{\frac{\gamma_a-1}{\gamma_a}}, \quad (3.1)$$

where p_{b1} – absolute pressure for combustion of unburnt hydrogen-air mixture in constant volume (as though after combustion it occupied the same fraction of the enclosure x_u). The given above model was validated against experiments by Stamps et al. (2006) and gave a good agreement with experimental data.

The transcendental equation, Eq. (3.1), was solved for overpressure in a sealed enclosure equal (p_2-p_0)=10kPa, which corresponds to the typical threshold value causing structural damage to civil structures. The range of studied hydrogen vol. fractions is 4-20%. Resulting solution is given in the Table 11. The table presents hydrogen vol. fraction in unburnt mixture x_{uH2}, volume fraction the unburnt mixture in the entire enclosure x_u, and "overall" volume fraction of hydrogen contained within flammability limits in entire enclosure $x_{H2} = x_{uH2} \cdot x_u$, which is a measure of hydrogen allowable to be safely released. The minimum for safely released hydrogen fraction is $x_{H2} = 0.314\%$ of total enclosure volume, assuming that all released hydrogen is at low flammability limit 4%.

Table 11. Solution of equation (3.1) for (p2-p0)=10 kPa.

x_{uH2}	x_u	$x_{H2} = x_{uH2} \cdot x_u$
0.04	0.0786	$3.14 \cdot 10^{-3}$
0.08	0.0474	$3.79 \cdot 10^{-3}$
0.12	0.0355	$4.26 \cdot 10^{-3}$
0.16	0.0293	$4.69 \cdot 10^{-3}$
0.20	0.0253	$5.06 \cdot 10^{-3}$

The maximum hydrogen inventory for non-destructive deflagration in enclosure may be calculated based on the conservative values of overall hydrogen fraction in enclosure 0.314% (vol.). The Table 12 below gives this hydrogen inventory volume and mass for a given enclosure volume.

Table 12. Solution of equation (3.1) for (p2-p0)=10 kPa.

Enclosure volume, m^3	1	10	100	1,000	10,000	100,000	1,000,000
H_2 volume, m^3	0.00314	0.0314	0.314	3.14	31.4	314	3140
H_2 mass, kg	$2.61 \cdot 10^{-4}$	$2.61 \cdot 10^{-3}$	$2.61 \cdot 10^{-2}$	0.261	2.61	26.1	261.0

The mass of hydrogen, therefore, may be approximated by a linear equation:

$$m_{H2} = 2.61 \cdot 10^{-4} V, \quad (3.2)$$

where m_{H2} is mass of hydrogen (kg), V is enclosure volume (m^3).

4.3.2 Vent sizing correlation for low strength equipment and enclosures (entirely filled in with flammable mixture)

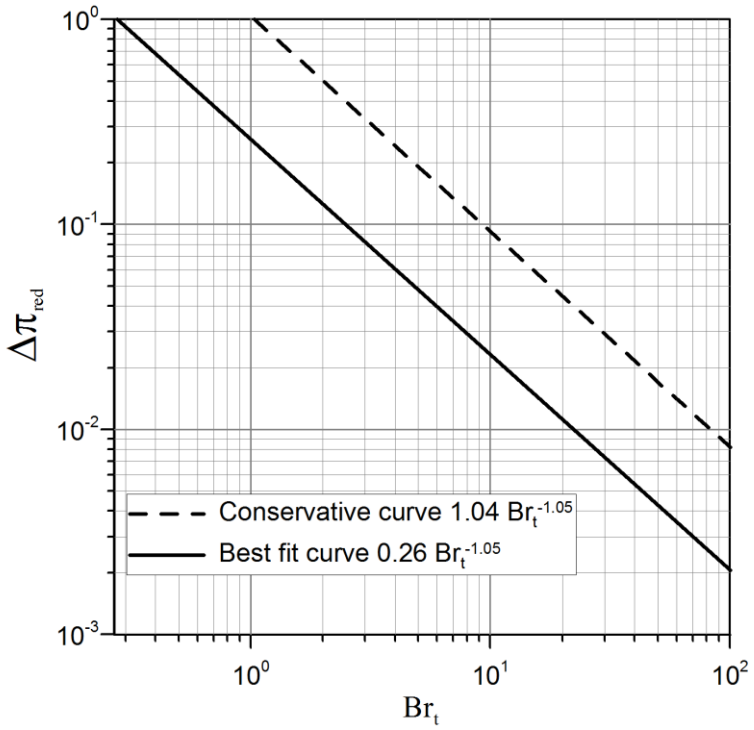

Figure 16. Vent sizing correlation for deflagration for low-strength equipment and buildings (Chernyavsky et al., 2014).

Figure 16 presents the vent sizing correlation (Chernyavsky et al., 2014) that can be used to calculate vent area required for the overpressure remaining below specified limit. The dimensionless overpressure is a function of turbulent Bradley number, Br_t. The best fit curve in Figure 16 is created using available experimental data, and the conservative curve is drawn in such a way that all available experimental data lies below it. Note that the correlation is derived for deflagrations in a low strength equipment and buildings, with deflagration overpressure not exceeding 1 bar.

The conservative correlation is

$$\Delta\pi_r = 1.04 \cdot Br_t^{-1.05} \tag{3.3}$$

where $\Delta\pi_r$ is the reduced overpressure and Br_t, is the turbulent Bradley number, can be used to calculate required vent area. The following procedure is applied to calculate vent area:

- Calculate the value of the dimensionless reduced explosion overpressure $\Delta\pi_r = (P_{max} - P_i)/P_i$, where P_{max} is the maximum allowable deflagration pressure and P_i is the initial pressure in the enclosure;
- Based on the value of $\Delta\pi_r$, calculate the value of Br_t by using the relevant equation (either best fit $\Delta\pi_r = 0.26 \cdot Br_t^{-1.05}$ or conservative $\Delta\pi_r = 1.04 \cdot Br_t^{-1.05}$):

$$Br_t = \left(\frac{\Delta\pi_r}{1.04}\right)^{-0.95} \tag{3.4}$$

- Calculate flame wrinkling factors as follows:
  - Calculate the Karlowitz wrinkling factor Ξ_K using equation

$$\Xi_K = 0.75 \cdot (E_i - 1)/\sqrt{3}\,. \tag{3.5}$$

where E_i is the combustion products expansion coefficient which can be obtained from Figure 17;

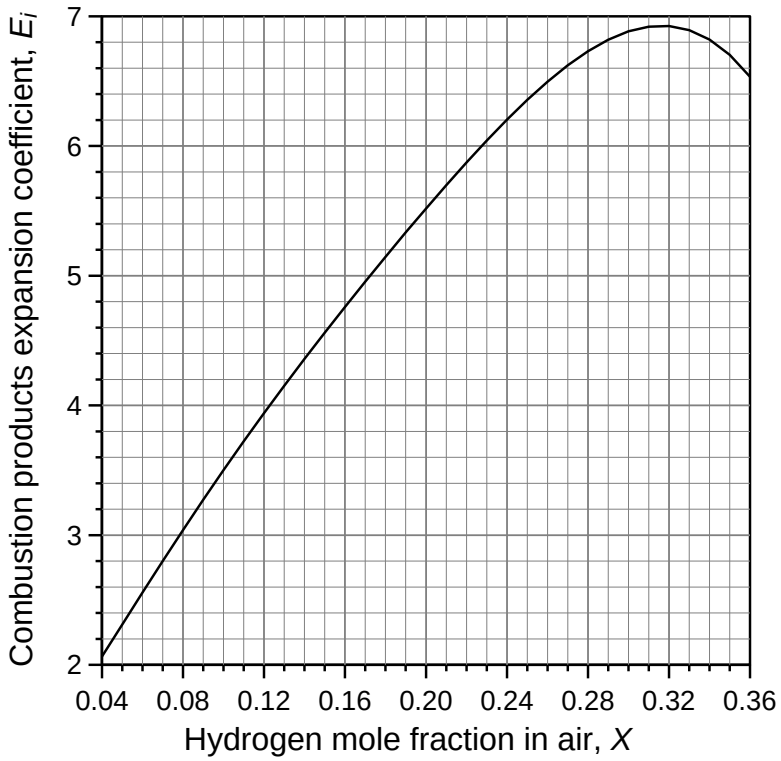

Figure 17. Combustion product expansion coefficient versus hydrogen mole fraction X (Verbecke, 2009).

- Find leading point wrinkling factor Ξ_{LP} from Figure 18;

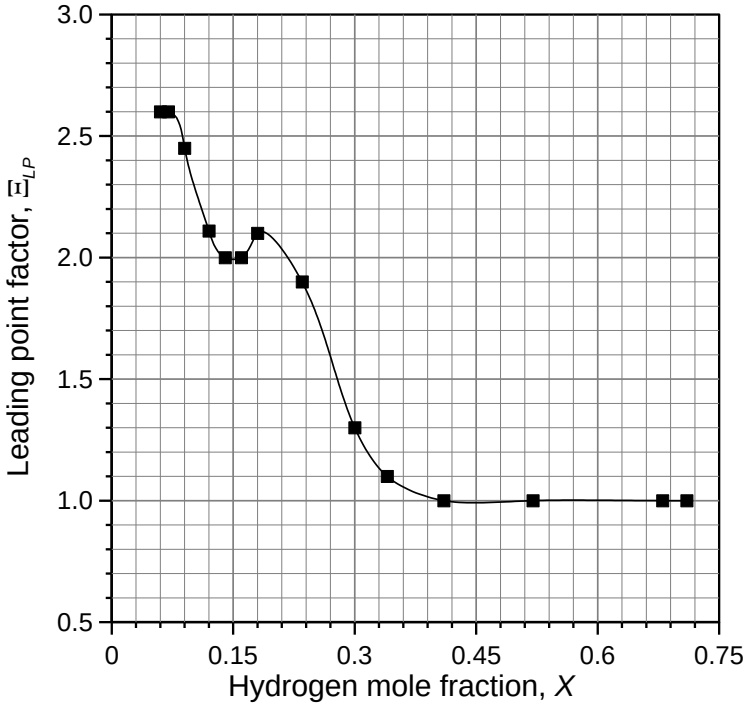

Figure 18. Leading point wrinkling factor versus hydrogen mole fraction X (Verbecke, 2009).

- Calculate wrinkling factor due to fractal increase of the flame front area Ξ_{FR}

$$\Xi_{FR} = \left(\frac{R}{R_0}\right)^{D-2} \quad \Xi_{FR} = \begin{cases} \left(\frac{R}{R_0}\right)^{D-2}; & R > R_0 \\ 1; & R < R_0 \end{cases}, \tag{3.6}$$

where $D = 2.33$ is fractal dimension (Bradley 1999), R (m) is the maximum flame radius $R = \sqrt[3]{3V/4\pi_0}$ (3.7) (Molkov and Bragin, 2013), where V (m^3) is the enclosure volume and π_0 is `pi` number = 3.1416, and R_0 (m) is the characteristic flame radius for transition from laminar to fully turbulent flame which can be calculated using formula

$$R_0 = \begin{cases} 4.3478 \cdot X - 0.2826; & 0.04 < X < 0.295 \\ 1; & 0.295 \le X < 0.75 \end{cases} \tag{3.8}$$

or by using Figure 19:

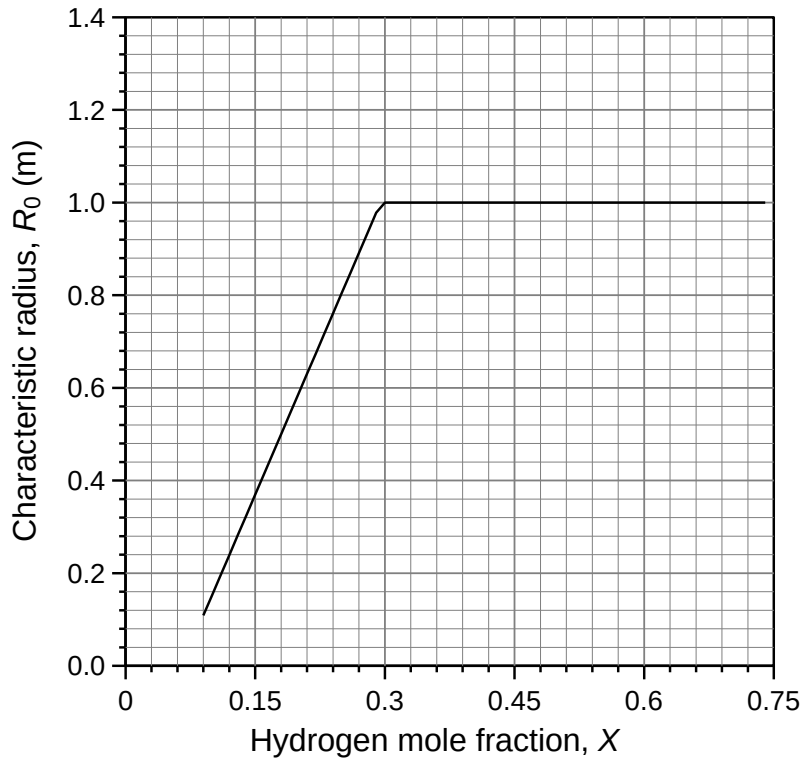

Figure 19. Characteristic flame radius for transition from laminar to fully turbulent flame versus hydrogen mole fraction X (Chernyavsky et al., 2014).

- Calculate aspect ratio wrinkling factor Ξ_{AR}

$$\Xi_{AR} = A_{EW} / A_S, \tag{3.9}$$

where A_{EW} (m^2) is the surface area of the internal enclosure walls and A_S (m^2) is the surface area of the sphere with the radius $R = \sqrt[3]{3V/4\pi_0}$ (Molkov and Bragin, 2013);

- Calculate wrinkling factor due to initial turbulence $\Xi_{u'}$. In order to do that it is necessary first to obtain "subgrid-scale" (SGS) wrinkled flame velocity S_w^{SGS} (m/s) which can be calculated as

$$S_w^{SGS} = S_u \cdot \Xi_K \cdot \Xi_{LP} \cdot \Xi_{FR} \cdot \Xi_{AR} \cdot \Xi_O \,, \tag{3.10}$$

where S_u (m/s) is laminar flame velocity and Ξ_O is the wrinkling factor due to the presence of obstacles, which in the absence of obstacles is assumed to be equal unity. Laminar burning velocity S_u can be obtained by correcting S_{u0}, taken from Figure 20 which is based on experimental data by Lamoureux et al., (2003) and Ross (1997), for initial pre-deflagration mixture temperature T_i (K)

$$S_u = S_{u0} \cdot \left(\frac{T_i}{298} \right)^{m_0} , \tag{3.11}$$

where m_0 is the temperature index which can be calculated using polynomial function

$$m_0 = -25.945589631 \cdot X^5 + 67.152094773 \cdot X^4 - 66.699205247 \cdot X^3 + 44.328192289 \cdot X^2 - \\ -18.547832349 \cdot X + 4.5752821336 \tag{3.12}$$

for $0.04 \le X \le 0.75$ (Verbecke, 2009), see also Table 13.

Table 13. Interpolated values of temperature index m_0 for selected hydrogen volume fractions (Verbecke, 2009).

X	15	20	25	29.5	35	40	43	45	50	55	60	65	70
m_0	2.6	2.2	1.9	1.7	1.5	1.45	1.4	1.4	1.45	1.5	1.7	1.9	2.2

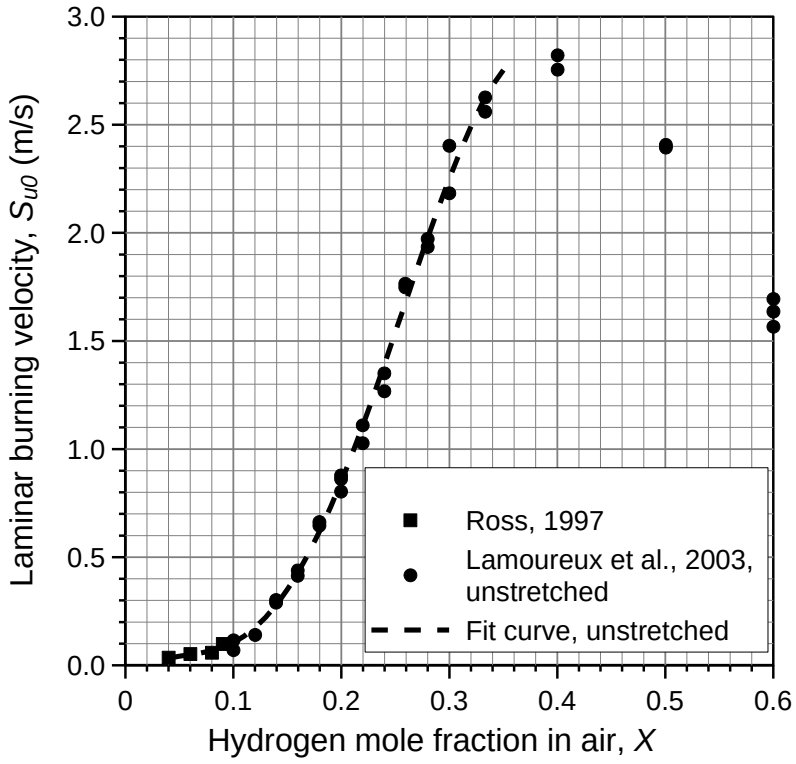

Figure 20. Laminar burning velocity Su versus hydrogen mole fraction X based on (Lamoureux et al., 2003; Ross, 1997) for initial temperature 298 K.

Once S_w^{SGS} is known it is possible to solve numerically transcendental equation (Molkov, 2012)

$$S_t = S_w^{SGS} \cdot \exp\left(\frac{u'}{S_t} \right)^2 , \tag{3.13}$$

in which S_t is the turbulent burning velocity due to initial turbulence and u' (m/s) is the RMS velocity in unburned mixture at the start of deflagration (equal to zero in quiescent mixture). This is a modified form

of Yakhot's original equation (Yakhot, 1988) modified to reflect the impact of all previously computed wrinkling factors (Molkov and Bragin, 2013). Finally wrinkling factor due to the impact of initial turbulence can now be computed as

$$\Xi_{u'} = S_t / S_w^{SGS}. \quad (3.14)$$

- With all wrinkling factors computed, it is now possible to calculate Deflagration-Outflow Interaction (DOI) number $\frac{\chi}{\mu}$ using the equation

$$\frac{\chi}{\mu} = \Xi_K \cdot \Xi_{LP} \cdot \Xi_{FR} \cdot \Xi_{u'} \cdot \Xi_{AR} \cdot \Xi_o; \quad (3.15)$$

- The next step is to calculate Bradley number B_r

$$Br = \frac{\sqrt[3]{36\pi_0}}{\sqrt{E_i / \gamma_u}} \cdot \chi / \mu \cdot Br_t, \quad (3.16)$$

where γ_u is the specific heat ratio of unburned mixture;

- Finally, the vent area can be determined using equation

$$F = Br \cdot V^{2/3} \cdot \frac{S_{ui}(E_i - 1)}{c_{ui}}, \quad (3.17)$$

where F is the vent area and c_{ui} is the speed of sound in the initial unburned mixture

$$c_{ui} = \sqrt{\gamma \frac{RT_i}{XM_{H_2} + (1-X)M_{air}}}, \quad (3.18)$$

where R=8.3145 ($J \cdot mol^{-1} \cdot K^{-1}$) is universal gas constant and M_{H_2} and M_{air} [kg/mol] are molar mass of hydrogen and air, respectively.

Example

Let us find the vent area required for deflagration of 18% hydrogen-air mixture (by volume) in the 1 x 0.98 x 0.96 m enclosure which would keep overpressure below 12 kPa.

1. Assuming that initial pressure in the enclosure is atmospheric ~ 100 kPa, $\Delta\pi_r = 0.12$;
2. From the conservative correlation Eq. (3.4) Br_t=7.780;
3. E_i for 18% hydrogen volume fraction is ~ 5.15 (Figure 17), giving from Eq. (3.5) $\Xi_k = 1.797$;
4. From Figure 18, $\Xi_{LP} = 2.1$;
5. In order to find Ξ_{FR} from Eq. (3.6) it is necessary first to calculate R and R_0. For the enclosure with the volume 0.94 m^3 R=*0.608* m (Eq. (3.7), R_0 = 0.5 from Eq. (3.8) and $\Xi_{FR} = 1.066$;
6. From Eq. (3.9) $\Xi_{AR} = 1.24$;
7. Let us assume that there is initial turbulence with $u' = 0.5$ in the enclosure (if initial turbulence is negligible, $\Xi_{u'} \equiv 1$. To find out $\Xi_{u'}$ it is necessary first to find S_u. From the Figure 20 $S_{u0} \approx 0.66$. Let the temperature prior deflagration equal 293K, than from Eq. (3.12) $m_0 \approx 2.35$ and from Eq. (3.11) $S_u \approx 0.63$. Multiplication of S_u by all previously found wrinkling factors provides $S_w \approx 3.17$ (Eq. (3.10)). Solving Eq. (3.13) numerically we obtain $S_t \approx 3.247$, and after substitution of S_t and S_w into Eq. (3.14) we obtain wrinkling factor $\Xi_{u'} \approx 1.024$;

8. Knowing all wrinkling factor coefficients it is now possible to calculate DOI number from Eq. (3.15): $\frac{\chi}{\mu} \approx 5.1$;
9. From Eq. (3.16), Bradley number $Br \approx 86.83$;
10. And finally, from Eq. (3.17), vent area $F \approx 0.5821\text{m}^2$.

This hypothetical example closely corresponds to one of the experiments performed at KIT (with exception of the presence of non-negligible initial turbulence in our example). Experimentally observed overpressure corresponded to $\Delta\pi_r = 0.12$ used in the example, but the vent area in real experiment was more than twice smaller (F=0.25 m^2), confirming conservative nature of the correlation Eq. (3.3).

4.3.3 Vent sizing correlation for the localized mixture deflagration

The vent sizing correlation for localised mixture deflagration in an enclosure was first developed theoretically in (Molkov, 1996) and recently validated against experiments performed at HyIndoor. The conservative correlation for localised mixture deflagration is:

$$\Delta\pi_r = 0.1\,Br_t^{-1.06}\left\{\frac{\sqrt{E_i/\gamma}\;E_i^{2/3}}{\sqrt{2}}\left(\frac{1+\left(\frac{1}{\varphi}-1\right)\frac{M_{air}}{M_{H2}}}{1+\left(\frac{1}{\Phi\varphi}-1\right)\frac{M_{air}}{M_{H2}}}\right)^{2/3}\right\}^{1.06} \tag{3.19}$$

where $\Delta\pi_r$ is the reduced (non-dimensional) maximum overpressure ratio, E_i is the combustion products expansion coefficient, γ = 1.4 is adiabatic index, Φ is volume fraction of combustible mixture in enclosure, φ is volume fraction of hydrogen in combustible mixture, M_{air} is molecular mass of air, M_{H2} is molecular mass of hydrogen, and Br_t is the turbulent Bradley number.

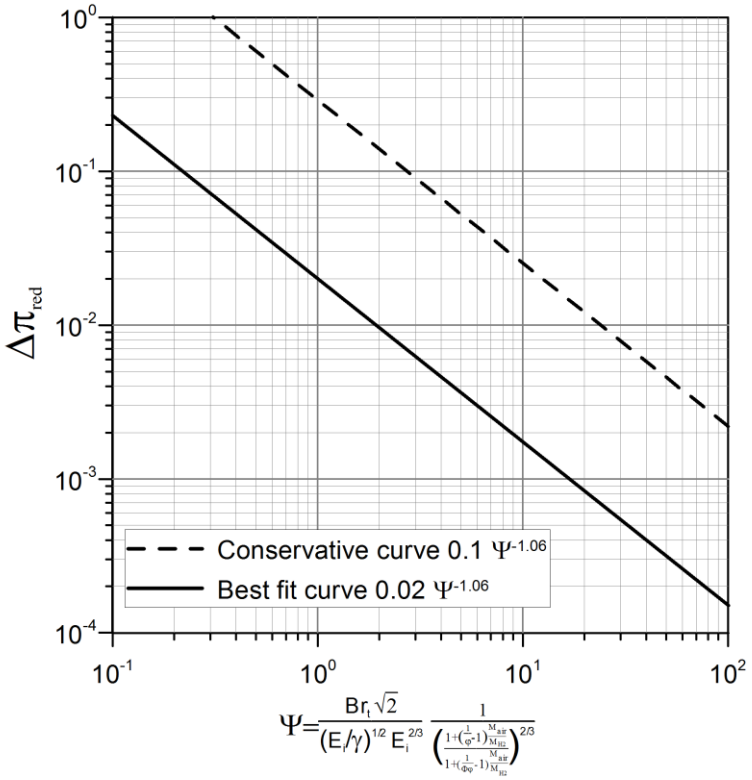

Figure 21. Vent sizing correlation for localized mixture deflagration.

Methodology to use the vent sizing correlation for localised mixtures (both uniform and non-uniform) is similar to that of the correlation for the case when uniform mixture occupies the entire volume of enclosure (see Appendix 4.3.2). The procedure for uniform localised mixture correlation calculation:

- Calculate the value of the desirable dimensionless reduced explosion overpressure $\Delta\pi_r = (p_{\max} - p_i)/p_i$ where $p_{\max}$ is the maximum allowable deflagration pressure and p_i is the initial pressure in the enclosure;
- For localized mixture with hydrogen distribution gradient:
  - Determine distribution of burning velocity S_{u0} (m/s) corresponding to hydrogen mole fraction in air X;
  - The fraction of the combustible mixture in enclosure Φ is accounted only as a portion of the total combustible mixture having burning velocity in the range (0.95÷1.0)S_{ui};
- Determine the appropriate value of combustion products expansion coefficient E_i from Figure 17 (for non-uniform mixtures use maximum hydrogen concentration);
- Based on the value of $\Delta\pi_r$, volume fraction of combustible mixture in enclosure Φ, volume fraction of hydrogen in combustible mixture and adiabatic index value γ = 1.4 calculate the value of Br_t by using the Eq. (3.19);
- Determine the values of burning velocity, sound speed and wrinkling factors:
  - temperature index m_0 can be found from Eq. (3.12) in Appendix 3.2 and laminar burning velocity S_{ui} from Eq. (3.11),
  - sound speed in combustible hydrogen-air mixture can be calculated as $c_{ui} = \sqrt{\dfrac{\gamma R T_i}{M_{air}\cdot(1-X)+M_{H_2}\cdot X}}$;
  - leading point wrinkling factor can be taken from Figure 18,
  - wrinkling factor Ξ_K from Eq. (3.5) $\Xi_K = \psi\cdot(E_i - 1)/\sqrt{3}$ using coefficient value $\psi = 1.0$,
  - characteristic radius of transition from laminar to fully turbulent flame R_0 can be found from

$$R_0 = \begin{cases} 4.3478\cdot X - 0.2826; & 0.04 < X < 0.295 \\ 1; & 0.295 \le X < 0.75 \end{cases}, \qquad (3.20)$$

  - radius of sphere of equivalent volume $R = [(3/4)\cdot(V/\pi)]^{1/3}$ (m) and wrinkling factor Ξ_{FR} from Eq. (3.6),
  - Ξ_{AR} from Eq. (3.9),
  - $\Xi_{u'}$ from Eq. (3.14),
  - Ξ_O is the wrinkling factor due to the presence of obstacles, which in the absence of obstacles is assumed to be equal unity, $\Xi_O = 1.0$,
  - Deflagration-Outflow Interaction (DOI) number χ/μ, from Eq. (3.15).
- Bradley number *Br* is calculated from Eq. (3.16) similar to that in section ”Vent sizing correlation for low strength equipment and enclosure”;
- The required vent area is found from Eq. (3.17) as $F = Br\cdot V^{2/3}\cdot S_{ui}(E_i - 1)/c_{ui}$.

Example:

Let us consider experimental enclosure with dimensions L × W × H = 1.0 × 1.0 × 1.0 m without obstacles. Hydrogen mole fraction distribution within enclosure height is given in Figure 22 (maximum hydrogen volumetric percentage is 15%). The combustible mixture is initially quiescent, $\Xi_{u'} = 0$. Mixture temperature is 20°C. Maximum allowable overpressure is $\Delta\pi_r = 3.0$ kPa.

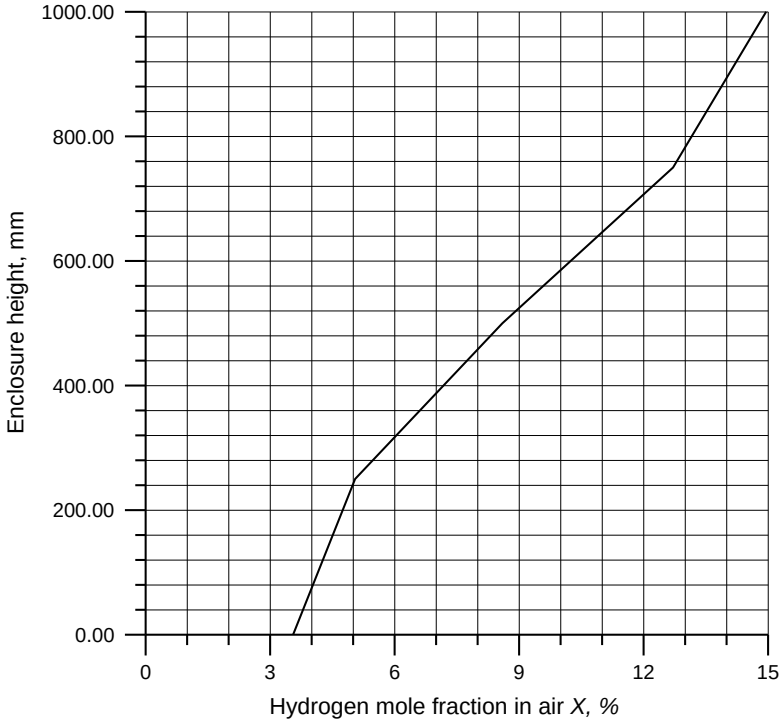

Figure 22. Distribution of hydrogen with enclosure height.

- Dimensionless reduced explosion overpressure $\Delta\pi_r = (p_{\max} - p_i)/p_i = 3000\,Pa/101325\,Pa \approx 3.0\cdot10^{-2}$.
  - Distribution of burning velocity S_{u0} within enclosure height corresponding to the given hydrogen distribution was obtained using data in Figure 20 and is given in Figure 23.
  - Maximum burning velocity is S_{u0} = 0.36 m/s, range of burning velocities (0.95 – 1.0)S_{u0} corresponds to velocity range S_{u0} = 0.34-0.36 and range of hydrogen fraction in the mixture (approximately) 14.5-15%, which occupies range of heights 0.97 – 1.0 m, giving volume fraction of unburnt mixture Φ=0.03.
- Combustion products expansion coefficient corresponding to the maximum hydrogen mole fraction φ=0.15 (from Figure 17) is E_i=4.55.
- Value of Br_t from the Eq.(3.19):

$$Br_t = \left(\frac{0.1}{\Delta\pi_r}\right)^{1/1.06} \frac{(E_i/\gamma)^{1/2} E_i^{2/3}}{\sqrt{2}} \left(\frac{1+\left(\frac{1}{\varphi}-1\right)\frac{M_{air}}{M_f}}{1+\left(\frac{1}{\Phi\varphi}-1\right)\frac{M_{air}}{M_f}}\right)^{2/3} = \left(\frac{0.1}{0.030}\right)^{1/1.06} \frac{(4.55/1.4)^{1/2}(4.55)^{2/3}}{\sqrt{2}} \left(\frac{1+\left(\frac{1}{0.15}-1\right)\frac{29}{2}}{1+\left(\frac{1}{0.03\cdot0.15}-1\right)\frac{29}{2}}\right)^{2/3} = 0.954$$

- Burning velocity, sound speed and wrinkling factors:
  - laminar burning velocity S_{u0} for the mixture in the enclosure from the Figure 20 is S_{uo}=0.36 m/s,
  - laminar burning velocity S_{ui} adjusted for initial mixture temperature from Eq. (3.11) using temperature coefficient m_0 = 2.6 from Eq. (3.12) is $S_{ui} = S_{u0}\cdot(T_i/298)^{m_0} = 0.36\cdot(293/298)^{2.0} = 0.34$ m/s,
  - sound speed in combustible hydrogen-air mixture $c_{ui} = \sqrt{\frac{\gamma RT}{29\cdot(1-X)+2\cdot X}} =$

$$= \sqrt{\frac{1.4\cdot8314\cdot293}{29\cdot(1-0.2)+2\cdot0.2}} = 380\,\text{m/s};$$

- leading point wrinkling factor Ξ_{LP} from Figure 18 is approximately $\Xi_{LP} = 2.0$,

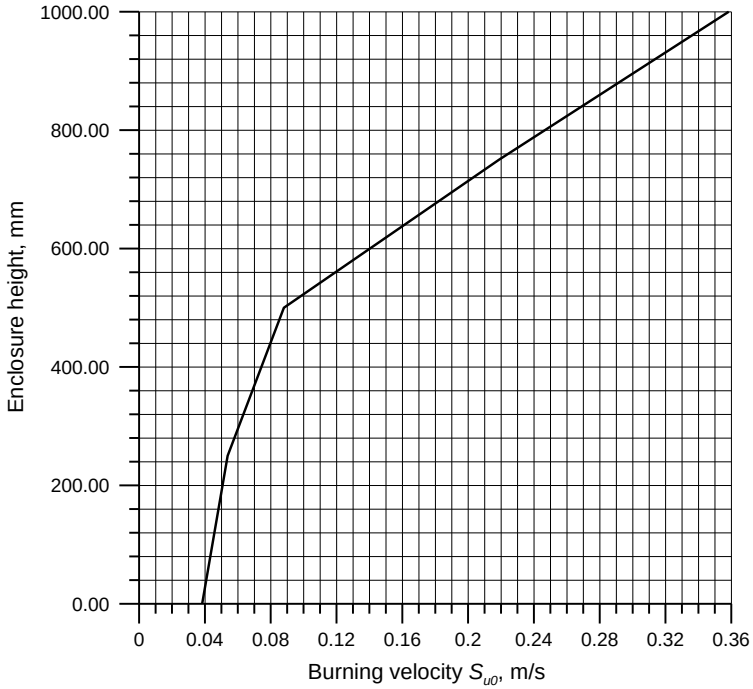

Figure 23. Distribution of burning velocity Su0 within enclosure height.

- wrinkling factor Ξ_K from Eq. (3.5) using coefficient value $\psi = 1.0$: $\Xi_K = 1.0 \cdot (E_i - 1)/\sqrt{3} = (4.55 - 1)/\sqrt{3} = 2.05$,
- parameters needed to find fractals and aspect ratio wrinkling factors: enclosure volume V=1.0 m^3; enclosure wall area is $A_{EW} = 6 \cdot 1.0 = 6.0\,\text{m}^2$; radius of equivalent volume sphere $R = [(L \cdot W \cdot H)/(4\pi/3)]^{1/3} = [(1.0 \cdot 1.0 \cdot 1.0)/(4\pi/3)]^{1/3} = 0.62\,\text{m}$; surface area of equivalent volume sphere $A_S = 4 \cdot \pi \cdot R = 2.26\,\text{m}^2$; radius for onset of self-similar flame propagation regime from Eq. (3.20) $R_0 = 0.36\,\text{m}$;
- fractal wrinkling factor from Eq. (3.6) $\Xi_{FR} = (R/R_0)^{D-2} = (0.62/0.36)^{0.333} = 1.20$ (equivalent sphere radius R is larger than radius for onset of self-similar flame propagation regime R_0 and fractals mechanism for flame wrinkling contributes to flame acceleration in this particular case);
- flame wrinkling accounting aspect ratio of enclosure from Eq. (3.9) $\Xi_{AR} = A_{EW} / A_S = 6.0/2.26 = 1.24$,
- initial mixture is not turbulized and quiescent, initial RMS velocity $u' = 0\,\text{m/s}$, flame wrinkling factor from initial turbulence from Eq. (3.14) $\Xi_{u'} = 1.0$;
- flame wrinkling due to the presence of obstacles is $\Xi_o = 1.0$;
- Deflagration-Outflow Interaction (DOI) number χ/μ, from Eq. (3.15)

$$\frac{\chi}{\mu} = \Xi_K \cdot \Xi_{LP} \cdot \Xi_{FR} \cdot \Xi_{u'} \cdot \Xi_{AR} \cdot \Xi_o = 2.05 \cdot 2.00 \cdot 1.20 \cdot 1.0 \cdot 1.24 \cdot 1.0 = 6.1.$$

- Bradley number from Eq. (3.16)

$$Br = \sqrt[3]{36\pi_0} \Big/ \sqrt{E_i/\gamma} \cdot \chi/\mu \cdot Br_t = \sqrt[3]{36\pi_0} \Big/ \sqrt{4.55/1.4} \cdot 6.1 \cdot 0.954 = 15.58$$

- Vent area from Eq.(3.23) $F = Br \cdot V^{2/3} \cdot [S_{ui}(E_i - 1)/c_{ui}] = 15.58 \cdot 1.0^{2/3}[0.344(4.55 - 1)/380] = 0.05$ m^2;

4.4 Appendix 4: Dealing with jet fires

4.4.1 Dimensionless flame length correlation

Figure 24 presents the dimensionless flame length $\frac{L_F}{D}$ correlation (Molkov, 2012; Molkov and Saffers, 2013), where D (m) is the nozzle diameter and L_F (m) is the flame length. It includes three regimes of fire: buoyancy-controlled jet or plume (left), momentum-dominated expanded jet (middle), momentum-dominated under-expanded jet (right). Variable X in the Figure 24 corresponds to the similarity group $\frac{\rho_N}{\rho_S}\cdot\left(\frac{U_N}{C_N}\right)^3$, where ρ is the density (kg/m^3), U is the velocity (m/s), and C is the speed of sound; subscript "N" designates parameters at the nozzle and subscript "S" designates parameters in the surrounding (ambient) air.
In order to be able to find dimensionless flame length, user must be able to calculate parameters included in the similarity group X. Therefore, the correlation requires application of the under-expanded jet theory (Molkov et al., 2009) in order to calculate under-expanded jet parameters at the nozzle exit, such as density, ρ_N, velocity U_N, and speed of sound C_N. This theory has been implemented and is available at the webpage of Cyber-laboratory at the website www.h2fc.eu.

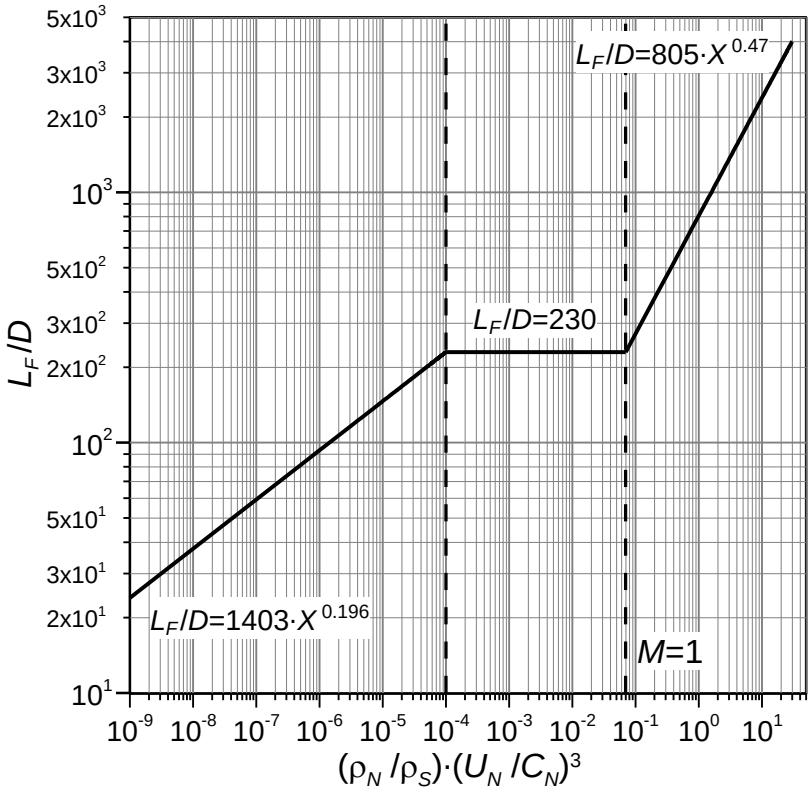

Figure 24. Dimensionless flame length correlation (Molkov and Saffers, 2013).

Example:
Let us consider hydrogen powered forklift in a warehouse which incorporates 350 bar storage tank at 293 K. When hydrogen is released through a 2 mm diameter the density of hydrogen in the nozzle exit, calculated by the under-expanded jet theory is 14.6 kg/m^3. The density ratio $\frac{\rho_N}{\rho_S}$ is 12.116 and the Mach number is 1. Having found the value of similarity group on the horizontal axis (X=12.116), we draw vertical line until it intersects with the correlation curve. Dimensionless flame length L_F/D can now be read from the vertical axis on the right. It is approximately equal to 2500. Knowing that the release diameter is 0.002 m, the dimensional flame length is approximately 5 m.

4.4.2 The effect of restrictor on the flame length

A flow restrictor is commonly located immediately downstream of high pressure storage in the pipeline. The flow restrictor will influence the flame length as will losses related to the pipe length. Friction losses are not considered, however it should be noted that they are proportional to $\frac{1}{D^4}$, where *D* (m) is the pipe diameter, so for an increased diameter frictional losses will be lower. For the under-expanded jet (Molkov and Saffers, 2013) obtained dimensional correlation $L_F = 76 \cdot (\dot{m}D)^{0.347}$, where L_F is the flame length (m) and $\dot{m}$ is mass flow rate (kg/s), which can be used to estimate the effect of restrictor on flame length, with mass flow rate taken as that at the smallest diameter.

The results of comparison of flame lengths with and without restrictor for several tank pressures and pipe diameters are provided in Table 14, in the assumption that the pipe failure occurred some distance from the restrictor. The flame would be even shorter if pipe ruptured immediately after the restrictor, in which case the reduction of flame length would be proportional to reduction of diameter, i.e. ratio of pipe and restrictor diameter.

The benefits of a restrictor can be clearly seen. For example for a 700 bar storage and a 25 mm pipe (as encountered in an existing refuelling station) the flame length without restrictor is 56 m. but when a 1 mm restrictor is utilized, the flame length is reduced to 6 m. Now if we used a 10 mm pipe with a 1 mm restrictor the flame length is reduced further to 4.3 m.

As a general rule of thumb, the effect of restrictor on the flame length can be estimated as:

$$\frac{L_f^{no\ restrictor}}{L_f^{restrictor}} = \left(\frac{D_f^{no\ restrictor}}{D_f^{restrictor}}\right)^{\frac{2}{3}} \quad (4.1)$$

Table 14. The effect of restrictor on flamelength

Storage pressure (bar)	Diameter (mm)	Restrictor diameter (mm)	Mass flow rate (kg/s)	Lf (m)
200	5	none	0.2282599	7.2398781
200	5	1	0.0091304	2.3694419
250	25	none	7.0009354	41.511453
250	25	1	0.0112015	4.4462877
350	5	none	0.3780851	8.6254101
350	5	1	0.0151234	2.822894
350	5	2	0.0604936	4.5667726
450	8	none	1.2018387	15.166747
450	8	1	0.0187787	3.5821849
450	10	none	1.877873	19.132678
450	10	1	0.0187787	3.8705775
450	10	2	0.0751149	6.2616759
450	15	none	4.2252142	29.180099
450	15	1	0.0187787	4.4553255
700	10	none	2.6929877	21.682279
700	10	1	0.0269299	4.3863665
700	10	2	0.1077195	7.0961002
700	25	none	16.831172	56.280825
700	25	1	0.0269299	6.0282339

4.4.3 Three deterministic separation distances for a jet fire

Three deterministic separation distances for a jet fire can be calculated based on the known jet flame length, L_F (m), (see Appendix 4.4.1) by using simple algebraic equations (Molkov 2012):

$X_1=3.5L_F$ (m) (“no harm” deterministic separation distance to temperature 70^{o}C)

$X_2=3L_F$ (m) (“pain” limit separation distance, temperature 115^{o}C for 5 min)

$X_3=2L_F$ (m) (third degree burns separation distance, 309^{o}C for 20 s)

4.4.4 Thermal radiation from a hot layer and ceiling during well-ventilated fire

Thermal radiation from a hot layer is not a trivial problem that requires knowledge of fire parameters such as temperature distribution in the layer and its thickness. To calculate the radiation heat flux from a hot layer of combustion products and ceiling surface such as metal sheet (for optically thin layers) the following calculation steps have to be taken:

1. Determine if your hot layer is optically thick or thin, e.g. using appropriate modelling tools. The hot layer of hydrogen combustion products is considered to be optically thick if the thickness is more than 1 m, and optically thin if thickness is less than 1 m.
2. Determine maximum temperature in the layer T_L (K) and the ceiling T_C (K) (the last applicable to only optically thin hot layers with thickness below about 1 m).

   The temperature of the steel sheet ceiling on the side of the enclosure is found from the Newton's law of cooling (Drysdale, 1999) $T_C = T_L - q''/h_L$, where T_C is the temperature of the steel sheet surface on the ceiling layer side K; T_L is the ceiling layer temperature under ceiling, K; h_L is the heat transfer coefficient in the ceiling layer inside the enclosure, W/(m^{2}K); $q'' = \frac{1}{\left(\frac{1}{h_L} + \frac{\Delta}{k} + \frac{1}{h_{amb}}\right)}\left(T_L - T_{amb}\right)$, where Δ is the thickness of the ceiling steel sheet, m; k is the thermal conductivity coefficient of the ceiling steel sheet, W/(mK); h_{amb} is the heat transfer coefficient on the ambient side of the ceiling steel sheet, W/(m^{2}K); T_{amb} is the ambient temperature, K.
3. Estimate partial pressure of water P_w in a hot layer, e.g. using CFD simulations
4. Calculate so-called a mean beam length by using equation L=1.8*L_T or L=3.6*(Volume of gas/surface area), where L_T is the layer thickness, m.
5. Calculate P_wL.
6. Use the nomogram in Figure 25 to calculate emissivity ε_L of the hot layer by knowing the partial pressure P_w, temperature T, and the mean beam length L for the gas volume geometry, at pressure P_e=1 atm.

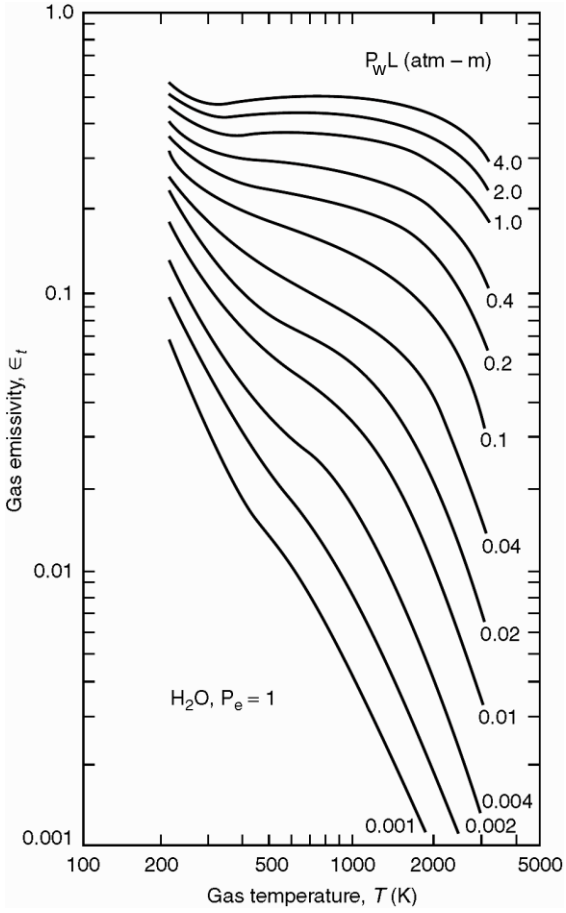

Figure 25. Emissivity of water vapour, adapted from (Tien C.L. et al., 2002).

7. Calculate shape factor F_{Lb} using the nomogram in Figure 26 or appropriate Eq. (4.2) or (4.3):

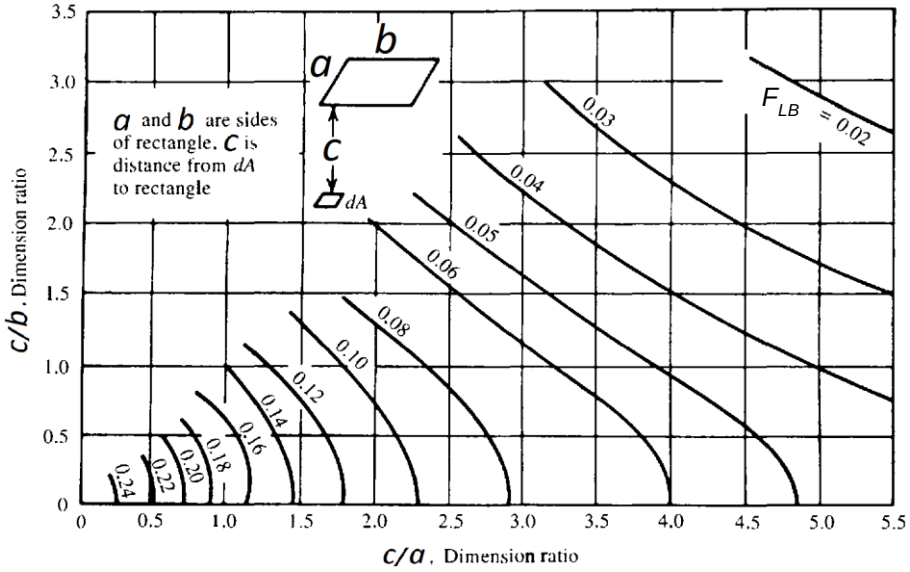

Figure 26. Shape factor FLb (Drysdale, 1999).

a. If receiver of thermal radiation (*dA* in Figure 27) is located parallel to radiating body (ABCD in Figure 27 left, and AB in Figure 27 right), e.g. configuration of a flash to the floor sensor and a hot layer under the ceiling, then shape factor is

$$F_{Lb} = \frac{1}{2\pi}\left[\frac{X}{\sqrt{1+X^2}}\tan^{-1}\left(\frac{Y}{\sqrt{1+X^2}}\right) + \frac{Y}{\sqrt{1+Y^2}}\tan^{-1}\left(\frac{X}{\sqrt{1+Y^2}}\right)\right], \quad (4.2)$$

where $X = a/c$, $Y = b/c$. (see Figure 27 for what parameters a, b, c stands for)

b. If receiver is located perpendicular to the radiating body, e.g. configuration of a flash to the wall sensor under the hot layer under the ceiling, then a shape factor is

$$F_{Lb} = \frac{1}{2\pi}[\tan^{-1}(1/Y) - AY\tan^{-1}(A)], \quad (4.3)$$

where $X = a/b$, $Y = c/b$, $A = 1/\sqrt{X^2 + Y^2}$.

Note:

If receiver is located not on the wall but somewhere under the radiating layer then it is required to add shape factors for each of four radiating section (see Figure 27, left): $F_{Lb_{total}} = F_{Lb_A} + F_{Lb_B} + F_{Lb_C} + F_{Lb_D}$.

If receiver located at the wall but not in the corner then two sections contribute to radiation (see Figure 27, right): $F_{Lb_{total}} = F_{Lb_A} + F_{Lb_B}$.

If receiver located at the corner there is only one section considered as contributing to radiation.

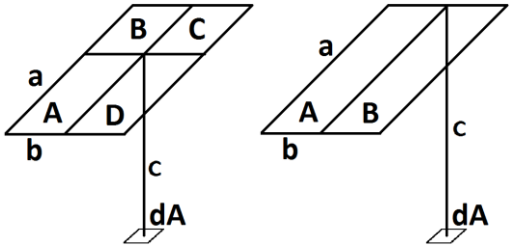

Figure 27. Illustration that shape factors additive.

8. Calculate thermal radiant heat flux q_R from layer and ceiling (the last is applicable to only optically thin layers) using the following equation:

   $$q_R = F_{Lb}\sigma\varepsilon_L T_L^4, \quad (4.4)$$

   where σ is the Stefan-Boltzmann constant σ=5.67·10^{-8} W/(m^2·K^4) and F_{Lb} is a shape factor, ε_L is the emissivity of the hot layer.

9. Sum up heat flux from layer and ceiling.mo

Example:

Let us consider the well ventilated case with 150 Nl/min release.

1. In experimental measurements the layer where the temperature was below 60°C was of 0.75 m thickness, it is less than 1 m so it is considered to be optically thin.
2. The maximum temperature in the layer was measured to be 395 K, the temperature in the ceiling can be calculated as:

   Assuming values of the heat transfer coefficients h_L=h_{amb}=5 W/(m^{2}K), thermal conductivity of carbon steel k=54 W/(mK), and steel sheet thickness as Δ=1 mm, the overall heat flux is

   $$q'' = \frac{1}{\left(\frac{1}{5W/(mK)} + \frac{0.001}{54W/(m^2K)} + \frac{1}{5W/(mK)}\right)}\left(395\,K - 278\,K\right) = 300\ W/m^2$$

   Then the temperature of the steel sheet surface on the ceiling layer side is $T_C = T_L - q''/h_L = 395\,K - 300\,W/m^2 / 5W/(m^2K) = 338\ K$.

3. Partial pressure of water based on experimental readings was 0.3.
4. The mean beam length is calculated by using equation L=1.8*L_T=1.8*0.75=1.35 (m).

5. Calculating $P_wL=0.3*1.35=0.41$.
6. Using the nomogram in Figure 25 to calculating the emissivity $\varepsilon_L=0.31$ of the hot layer by knowing the partial pressure $P_w=0.3$, temperature $T=395$ (K), and the mean beam length $L=1.35$ (m). The emissivity for the ceiling was considered as a grey body of 0.95.
7. Since the sensor was located on the floor close to the middle of the enclosure Eq. (4.3) was applied to calculate the individual shape factor for the layer and the ceiling by knowing the coordinates of the sensor. The shape factor for the layer to sensor (body) is F_{Lb}=0.49, shape factor ceiling to the sensor (body) is $F_{Cb}=0.34$.
8. Calculating thermal radiant heat flux from layer $q_R = F_{Lb}\sigma\varepsilon_L T_L^4$=0.49*5.67·10^{-8} * 0.31 * 395^4=210(W/m^2) and ceiling $q_R = F_{Lb}\sigma\varepsilon_L T_L^4$=0.34*5.67·10^{-8} * 0.95 * 338^4 = 237(W/m^2)
9. Summing up the thermal radiant heat flux both from the layer and from the ceiling to get the total heat flux q_R=210+237=447 (W/m^2).

4.5 Appendix 5: Sensor recommendations for some indoor applications

4.5.1 Forklift vehicle operation and refuelling in a warehouse

Fuel material handling vehicles such as forklifts have been deployed in many industrial sites. Although not mandatory, the vehicles themselves typically have on-board hydrogen sensors as part of their safety system (Buttner et al., 2012). The use of chemical sensors to monitor the hydrogen dispenser may be mandatory, depending on the locally applicable regulations. Hydrogen sensors are mounted close to the hydrogen dispenser either on the wall adjacent to and above the dispenser or on the ceiling above the dispenser. Typically a single sensor is used (Buttner et al., 2012). The indoor refuelling of materials handling vehicles in a warehouse is at present not to be covered in standard ISO WDTR 19880-1 for gaseous refuelling stations, which is currently under development, but may be included in the future. The combustible gas detection system should trigger an alarm at 25 % of the lower flammability limit (LFL) and shut down the power system fuel supply at 50 % of LFL, respectively.

Sensors should normally be located as high as possible, but accessibility for calibration/maintenance should be taken into account, and the distance to a potential leak source should be considered as well. Depending on the ceiling structure, compartments where hydrogen can be accumulated should be monitored carefully. Placement of the sensor near doors or other openings should be avoided as hydrogen could be diluted.

In a warehouse setting, some variations in temperature, relative humidity and gas flow (in case of natural ventilation) can be expected. All these parameters influence the sensor performance (Palmisano et al.[1], 2014), in some cases significantly. Extremely high temperatures are unlikely as for persons working in the warehouse a comfortable range of 13-25°C is likely to be a target, but in the summer temperatures of up to 40°C could be reached. In addition, for refrigerated rooms the suitability of the sensor for freezing conditions should be ascertained for the hydrogen sensors. The temperature dependence of the sensor sensitivity should therefore be carefully considered. As a hydrogen sensor is likely to be placed near the roof, the vertical distribution of air temperature should be considered. In a warehouse a maximum increase of temperature of 0.9°C/m can be reached (Porras-Amores, 2014). As this variation could affect the sensor performance, the sensor should therefore be calibrated in-situ. In case of high ceilings, layers of heated air may form, which may act as a thermal barrier to gas diffusion. Diurnal and seasonal temperature variations can also be expected in a warehouse. Very high relative humidity or even condensing conditions are unlikely to be encountered in this setting, as moisture should be avoided for storage of goods.

The likely pressure range will be within normal range of the Earth's air pressure 980 millibars (mb) to 1050 mb, with possible overpressure in protected environments. Flow may be one of the most critical variables in case of natural ventilation, which could be highly variable. The indoor air renewal in the warehouse can be either by natural ventilation through the doors or forced ventilation, which will affect the flow rate of air. Normally drafts should be kept below 1.5m/s to prevent possible discomfort to workers, therefore high flow rates above 1m/s are not expected. However low flows are possible and it should be ascertained that the sensor is not placed in an area with insufficient ventilation. A careful analysis of ventilation patterns before placement of the sensor is therefore advisable.

Many potential contaminants could be present in a warehouse setting, especially NOx and CO from the combustion engines of conventional ICE fork lift trucks in case of mixed fleets. In addition, siloxanes from the use of lubricants and sealants are likely. In refrigerated warehouses ammonia or chlorofluorocarbon compounds may be released (Buttner et al., 2012). Regulatory bodies state permissible exposure limits for a large number of potential contaminants to protect human health, but even lower levels may affect the sensor performance(Palmisano et al.[2, 3], 2014).

Of the three sensor types tested in the HyIndoor project, the thermal conductivity sensor fulfils all requirements of this specific application, due to their stability to temperature variations, low dependence on flow and resistance to contaminants. Other sensor types could be used, but the robustness of the sensing platform needs to be considered. Both EC and MOX sensors could be inherently sensitive to poisoning (Palmisano et al.[3], 2014; Korotcenkov and Cho, 2011). Many manufacturers employ protective measures to protect the sensor against poisoning. Other sensor platforms may be used for this application, but were not analysed further in the scope of this study. It may be mandatory to use a sensor with ATEX protection, depending on the zoning.

4.5.2 Small scale reformer

Hydrogen can be provided close to the site of use through small scale reformers. The reformer is typically housed within container or other structure to provide protection from the environment. The safety system will encompass flow regulators and shutoff valves, but hydrogen sensors may be used to provide additional safety. The hydrogen generator is based on the reformation of methane (CH_4) to hydrogen. The reaction generates H_2O, CO and CO_2 as secondary products. H_2, CH_4 and CO are all flammable species and their release could cause a hazard.

The hydrogen generator could be regarded as a closed room in which different vessels containing flammable gases are located. Typically these systems are housed inside a 20 or 40 foot container, with dimensions in the range of 15 – 30 m^3 with a ceiling 2.5 m high. During normal operation the container is highly ventilated, but may rely on natural ventilation during a stand-by or a shutdown period. The different vessels retain operating pressure during shutdown periods.

Small leakages may be present in the proximity of gaskets and tubing connections. To prevent dangerous situations, H_2 sensors and CO sensors could be deployed. In general, combustible gas sensors are suggested for this application. The most commonly used platforms for sensing combustible gases are MOx and CAT. MOx sensors are very sensitive, but are somewhat lacking in linearity and robustness. Due to their better linearity and improved stability, CAT sensors were identified as the most suitable platforms for this application. The positioning of the sensor shall be on the ceiling. ATEX protection may be required. Sensor resistance to sulphur compounds is favourable for this deployment. Of the 5 platforms tested the 2 CAT sensors with ATEX protection were identified as the most suitable for this application.

4.5.3 Fuel cell for back-up power generation

Some facilities and installations need to be equipped with a back-up power supply, such as hospitals and telecommunication towers. Fuel cells have proven to be well suited to this application and are deployed for this purpose. Depending on the application and the size/power of the fuel cell, it can be either placed indoors or outside in a dedicated container. The safety of stationary fuel cell power systems is covered in IEC 62282-3-100. Indoor placement of a fuel cell may require an automatic shutoff valve interlocked with gas detection for fuel sources located outdoors and serving an indoor fuel cell power system (e.g. NFPA 853, 2010)

4.5.4 Fuel cell container

The fuel cell container is a confined space usually placed outdoors, thus, environmental parameters such as relative humidity and temperature can vary remarkably.

Although the analysis undertaken in HyIndoor shows that this application does not present a critical scenario [citation needed], the use of H_2 sensors for detecting the presence of leakages is suggested. Reliable, sensitive and robust (with respect to environmental parameters) hydrogen sensors are needed in this case. A gas detector, which is mandatory for the fuel cell power system, shall comply with ISO 26142 or IEC 60079-29-1, as appropriate. A combustible gas detection system shall be installed in the fuel cell power system enclosure or fuel cell power system exhaust system or in the container containing fuel cell power system installations. Location of gas detection systems in the container shall be chosen to provide the earliest warning of the combustible gases present. Location of gas detectors shall be in accordance with IEC 60079-29-2. The combustible gas detection system shall be arranged to alarm at 25 % of the lower flammability limit (LFL) and be interlocked to shut down the power system fuel supply at 50 % of LFL, respectively. The LFL used shall be the lowest flammability limit of the gas or gas mixtures.

The sensor deployed should allow for measuring hydrogen in a wide concentration range and show high resistance to poisoning. The power consumption of the sensor should be carefully considered for remote locations with grid power supply.

4.5.5 Fixed indoor hydrogen energy based system

A stationary fuel cell system placed indoors should comply with all applicable building regulations. The storage of hydrogen is outside the fuel cell cabinet, either located outdoors or in a dedicated storage facility. Within the HyIndoor project, several risk mitigation strategies were discussed, such as the possibility of adding passive vents (see 1.2.5). In case this is not possible it may be necessary to either have continuous ventilation or to add a gas detection system. In the latter case, neither large variations in temperature or relative humidity are expected, and forced ventilation should provide sufficient flow. Other than the general considerations outlined above, no particular requirement for the sensor need to be taken into account, but depending on the zoning, ATEX protection may be necessary.